Cleveland State University
EngagedScholarship@CSU

ETD Archive

2009

Probabilistic Stress Analysis of Liquid Storage Tank

Khader A. Khan
Cleveland State University

Follow this and additional works at: https://engagedscholarship.csuohio.edu/etdarchive

Part of the Mechanical Engineering Commons

How does access to this work benefit you? Let us know!

PROBABILISTIC STRESS ANALYSIS OF LIQUID STORAGE

TANK

KHADER A. KHAN

Bachelor of Engineering in Mechanical Engineering

Jawaharlal Nehru Technological University, India

May, 2005

Submitted in partial fulfillment of requirements for the degree

MASTER OF SCIENCE IN MECHANICAL ENGINEERING

At the

CLEVELAND STATE UNIVERSITY

December, 2009

This thesis has been approved

for the Department of MECHANICAL ENGINEERING

and the College of Graduate Studies by

_____

Thesis Committee Chairperson, Dr. Rama S. R. Gorla

_____

Department and Date

_____

Dr. Earnest N. Poulos

_____

Department and Date

_____

Dr. Asuquo B. Ebiana

_____

Department and Date

ACKNOWLEDGEMENT

PROBABILISTIC STRESS ANALYSIS OF LIQUID STORAGE TANK

KHADER A. KHAN

ABSTRACT

Liquefied Natural Gas transport and storage has become very important due to its ability to occupy $1/600^{th}$ of the volume that compressed natural gas would occupy at room temperature and atmospheric pressure. In the present work, an LNG storage tank has been computationally simulated and probabilistically evaluated in view of the several uncertainties in the fluid, structural, material and thermal variables that govern the LNG storage tank. A finite element code ALGOR was used to couple the thermal profiles with structural design. The stresses and their variations were evaluated at critical points on the storage tank. Cumulative distribution functions and sensitivity factors were computed for stress responses due to fluid, mechanical and thermal random variables. These results can be used to quickly identify the most critical design variables in order to optimize the design and make it cost effective. The total heat gained by the liquid part in the tank has been evaluated and the amount of boil-off was calculated. Various methods have been proposed to minimize thermal stresses.

TABLE OF CONTENTS

LIST OF TABLE

LIST OF FIGURES

NOMENCLATURE

LNG   Liquefied Natural Gas

g   Acceleration due to gravity

α Thermal expansion coefficient of the fluid

L Distance between the temperature difference

T_i inside temperature [^{0}C]

T_o Ambient Temperature [^{0}C]

ν Poisson's ratio

μ Dynamic viscosity of the fluid

ρ Density of the fluid

c_p Specific heat of the fluid

K Thermal conductivity of the fluid

p internal pressure of the tank [Pa]

D inside diameter of a tank [m]

h_o outside heat transfer coefficient

Re Reynolds number

Pr Prandtl number

Nu Nusselt number

E Young's modulus of elasticity

t Thickness

h_i inside heat transfer coefficient

ε emissivity

σ	Stefan–Boltzmann constant
ϕ	Galerkin shape function
Ψ	Galerkin weight function
θ^e	Element nodal load distribution
q''	Thermal radiative heat flux
F_{rad}	Radiation view factor

CHAPTER I

INTRODUCTION

Natural gas is one of the most effective means of coping with today's energy crisis. It has many applications for domestic purposes such as heating, electric generation in power plants and powering vehicles. The demand of natural gas has increased 5 times in the last few decades [1]. This demand is due to the fact that natural gas is easily transportable and environmentally friendly.

Chen *et al*. [2] predicted the temperature and pressure changes in liquefied natural gas cryogenic tank. The properties and composition of LNG fuel were simulated inside the tank as a function of time. Boil off is defined as the gas being released from the liquid. Boil off of LNG in these LNG tanks usually takes place at LNG stations and can cause excessive pressure build up in LNG tanks. Boil-off is caused by heat added to LNG fuel during the storage and the filling processes. Heat can leak through the shell of the tank, and be added to the LNG fuel during the operation. They stated that the boil-off of the LNG is mainly due to the heat gained by the tank from outside ambient temperature. Also, the heat leakage into the tank leads to increase the vapor pressure. Their experiment showed the percentage of LNG which needs to be boiled off in order to reduce the vapor pressure. Natural gas is stored in a liquefied state at a temperature as

low as -162^0 C in order to decrease its volume and to facilitate transportation. In its liquid state, the density of natural gas is 600 times more than Compressed Natural Gas (CNG) at room temperature and atmospheric pressure [2]. Compressed natural gas is typically stored at pressures up to 24.821 MPa in cylindrical steel tanks.

In order to reduce boil-off, Liquefied Natural Gas (LNG) should be stored in special tanks which have multi-layered insulation that minimize heat leakage. There are three different classifications for liquid natural gas (LNG) storage tanks [3]: single containment, double containment, and full containment. A single containment tank is either a single tank or a tank consisting of an inner and an outer tank such that only the inner tank is capable of storing the LNG. A double containment tank is defined as having an inner and outer tank that is both capable of independently containing the LNG. A full containment tank is defined as a double tank in which the outer tank of a full containment tank is capable of both containing the liquid cryogen and of controlled venting of the vapor of the cryogen after a leak.

Tanks are additionally classified by the elevations from the ground level: above-ground type, in-ground type and under-ground type. The type of tank treated in this study is an above-ground full containment type tank. Generally, LNG storage tanks are composed of three parts: inner tank, outer concrete wall and roof. According to the shape of the inner tank, there are two types of LNG storage tank: 9%-Ni type and membrane type [4]. The 9%-Ni type has a self-supporting inner tank which endures the thermal contraction of LNG temperature, and the hydrostatic pressure from the weight of the LNG.

Jeon *et al*. [5] applied a special method to predict the temperature of the inner walls of the insulation. In their proposed model, the effects of the outer tank, the insulation layer and a

suspended deck were considered. The geometrical dimensions of the tank and the properties of the material used in the tank can be found in this reference.

During normal operation, the inner tank is exposed to cryogenic temperatures from the LNG. However, if LNG leaked from the inner tank, it would soak into the insulation. In the event of such an accident, some insulation layers would not be able to function, and the outer concrete tank could be structurally compromised by a quick temperature drop [3]. In conclusion, the safety of the tank can be ensured only through a thorough thermal analysis.

Graczyk *et al*. [6] performed a probabilistic analysis of the sloshing-excited tank pressures in LNG tankers. They found that ship motion results in violent fluid motion in the tank which causes high tank pressure. The pressure was measured in a series of a model tests, and the important issues of structural responses, such as the significance of spatial and temporal characteristics of sloshing loads as well as the model scaling problem were addressed.

Design specification of the tank has to be studied thoroughly in order to do a simulation of the storage tank. The properties of all the parts of a storage tank have been described by Jeon and Park [7]. They discussed safe and economical construction for the above-ground LNG tanks. As the capacity increases, special attention needs to be given to the design code and an efficient procedure needs to be established to design an LNG tank with structural and cost efficiency.

Various analyses have been carried out by KOGAS technology [8], including static analysis, wind loading, modal and seismic analysis, temperature modeling, leakage modeling, pre-stress/post tensioning, burn-out modeling, relief valve heat flux modeling and soil-structure interaction. They used the LUSAS finite element modeling software to design a 200,000 m ^{3} above ground tank. They considered a 2D axisymmetric model for the static stress and thermal

analysis, and 3D shell elements for modal analysis and seismic analysis. For burn-out modeling, they performed a transient thermal analysis and predicted the time required for the fuel to burn out completely.

Natural convection causes circulation of the LNG within the storage tank which tends to maintain a uniform liquid composition. The addition of new liquid can result in the formation of strata of slightly different temperature and density within the LNG storage tank. "Rollover" refers to the rapid release of LNG vapors from a storage tank caused by stratification. The potential for rollover arises when two separated layers of different densities (due to different LNG compositions) exist in a storage tank. LNG rollover phenomena received considerable attention following a major unexpected venting incident at an LNG receiving terminal at La Spezia, Italy in 1971 [9]. The main hazard arising out of a rollover accident is the rapid release of large amounts of vapor leading to potential over-pressurization of the tank. It is also possible that the tank relief system may not be able to handle the rapid boil-off rates, and as a result the storage tank will fail leading to the rapid release of large amounts of LNG.

Salem and Gorla [10] performed a probabilistic finite element thermal analysis of a water tank to determine critical design parameters and to perform design optimization. Thacker and a team of researchers [11] at the Southwest Research Institute described the development of the NESSUS probabilistic engineering analysis software. Gorla et al. [12] performed the first probabilistic study that interconnected computational fluid dynamics and finite element structural analysis. In this study a combustor liner was simulated by using the finite element method and evaluated probabilistically. The inlet and outlet temperatures were found to greatly influence the hoop stress. Gorla and Gorla [13] performed a probabilistic analysis of a non-gasketed flange. Cumulative distribution functions and sensitivity factors were computed for heat loss due to 11

4

random variables. Gorla and Haddad [14] performed a finite element heat transfer and structural analysis of a cone-cylinder shell pressure vessel. They presented sensitivity factors for the stress versus the random variables.

The objective of the present work is to design a robust LNG storage tank system which continues to function well when the operating conditions are not ideal. The location and magnitude of the maximum thermal stress was evaluated using a finite element axisymmetric model of the tank in ALGOR, a FEA package which performs design analysis, simulation and the optimization. The maximum von Mises stresses, and cumulative distribution functions and sensitivity factors of stress were evaluated for the 54 random variables varied by ± 10 %. The maximum boil-off in terms of weight percent per day of the entire tank LNG weight was evaluated at the mean value of the random variables.

CHAPTER II

PROBLEM STATEMENT

Cryogenic tanks generally have an inner and outer wall. Nine percent nickel steel is widely used as a material for the inner tank since it has sufficient strength and toughness for cryogenic applications [4]. The 9% Ni steel inner tank and the outer tank are isolated by super insulation. The heat that leaks into such tanks is measured as a percentage of boil off of total tank volume per day. For a storage tank, the boil-off rate ranges from 0.05% to 0.1% in total tank volume per day depending upon the type of cryogen and the quality of the insulation of the tank [8]. The heat that leaks into the cryogenic tank vaporizes a certain amount of liquid that changes the pressure in the tank which in turn significantly influences the properties of the cryogens. The present work contains an approach to accurately calculate the amount of heat that leaks into the tank by using the ALGOR FEA code. Fifty four random variables are considered in this analysis which are defined later in this chapter.

In the LNG storage tank, rendered in Figure 1, the inside temperature is taken to be -162 ^{0}C and the outside ambient temperature for this analysis is conservatively taken to be 35 ^{0}C. Heat enters from outside the tank to the liquid through conduction, convection, and thermal radiation all of which are treated in the finite element analysis.
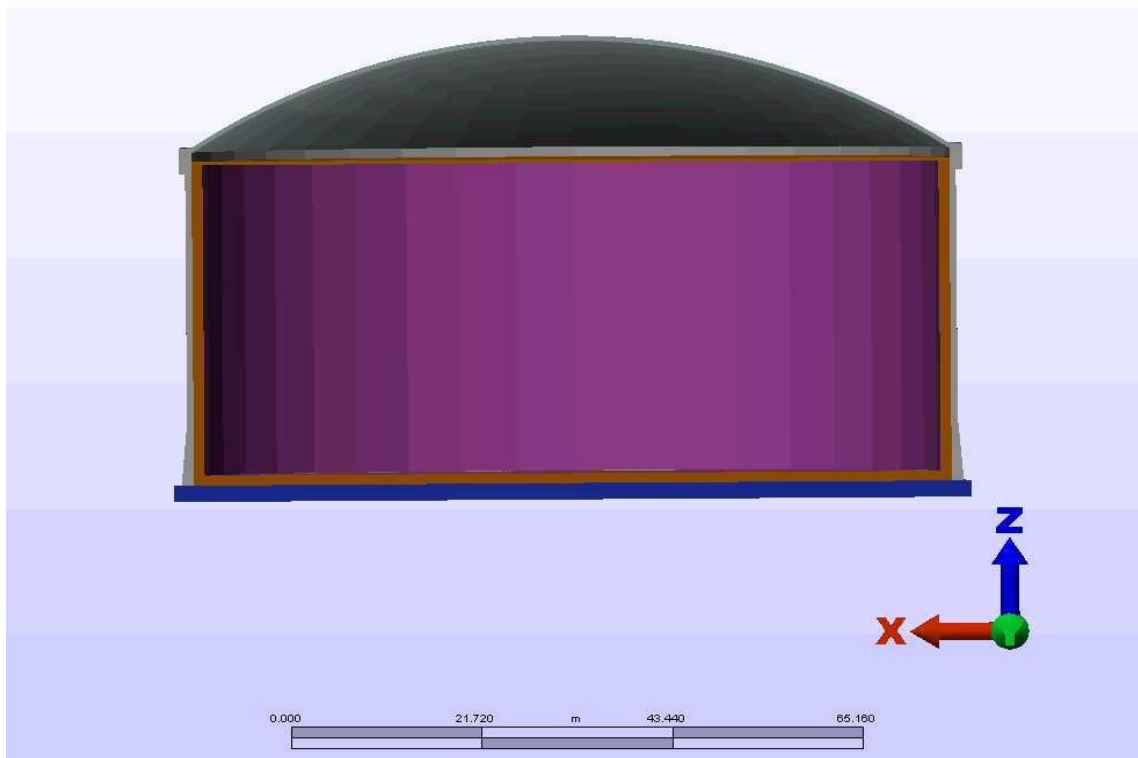
Figure 1. Rendering of LNG tank in ALGOR.

The main components of the LNG tank are the inner tank, outer tank, roof, suspended deck and the concrete base as shown in Figure 2. The inner tank is made of 9% Ni steel which is 50 mm thick in this study. The liquid cryogen is in direct contact with inner tank [4]. In case of leakage, the cryogenic liquid comes in contact with the outer wall. The outer tank is made of concrete having a tapered design starting at 1.4m thick at the bottom reducing to 0.7m thick at the top. The taper is specified to enable the tank to withstand the higher stresses acting at the bottom.

The modes of heat transfer from the environment to the LNG tank are convective heat transfer between the outer tank wall and the surrounding air, conduction through the outer wall and the inner wall, and then convection between the inner wall and the cryogenic fluid takes

place. An air gap exists between the roof of the tank and the suspended deck which was specified to reduce conduction heat transfer. Thermal radiation heat transfer occurs in this air gap. The concrete base is 2m thick and it sits on steel piles and the ground temperature is 35°C. These different modes of heat transfer contribute to the thermal stresses in the LNG tank. LNG internal pressure produces the main loadings of the wall.

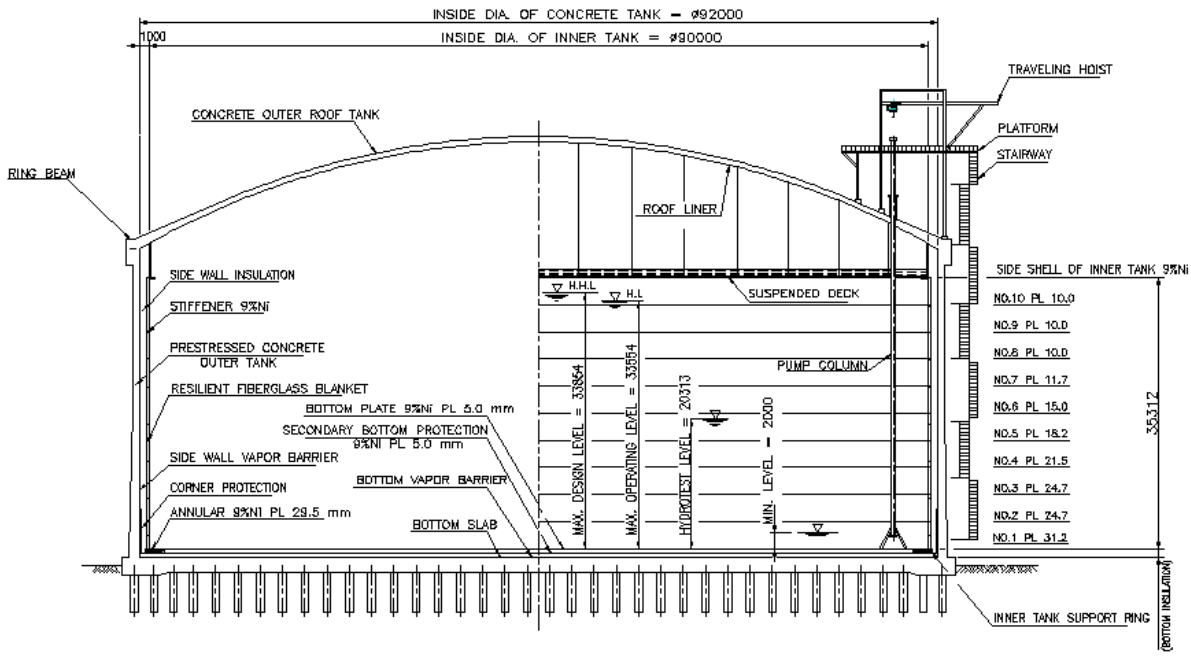Figure 2. Drawing of LNG storage tank.

DESIGN OF OUTER TANK

LNG outer tank is divided into structural components and each component is separately investigated. This approach is expected to give insights into the sizing problem prior to the

8

detailed analysis of whole structure when the capacity expansion is attempted. Below, the parts of the LNG outer tank are introduced.

Roof dome

Many of the existing concrete roof domes of above-ground LNG tanks have the radius of curvature equal to the diameter of outer wall. The dome corresponds to the rise to diameter ratio of 1 to 8, which is often recommended for the roof domes where self-weight and/or externally distributed load are dominant. Those practices may originate from the elementary membrane theory, since no tensile stress is induced in hoop direction under those kinds of loads for flat domes with that rise or less. On the other hand, it can be detected that a higher rise is advantageous in the structural aspect when subjected to internal pressure, since the higher curvature can endure internal pressure with lower tensile stresses. Therefore, it can be said that when the internal pressure is additionally considered, which is one of the main design loadings in LNG tanks although the magnitude is far smaller than that in the nuclear containment structures, conventional rise of the domes in the above-ground LNG tanks is not optimal at least in terms of structural safety.

In designing the LNG tank with 200,000 m^3 capacity the rise of dome should not be more than 0.8d in order not to violate the American Petroleum Institute (API) code, where d is the diameter of outer wall. Besides structural safety, no special code-related restriction is imposed on the shape of concrete dome. However, the codes for the carbon steel liner that is attached inside the concrete dome should be followed as well. The code API 650 specifies that radius of curvature of the liner should range from 0.8d to 1.2d. Some of the large in-ground LNG tanks

where the roof dome is also exposed above the ground level had the radius of curvature close to 0.8d.

Structural safety check should be performed in two ways for the concrete domes, i.e., with respect to the allowable stress and buckling. Buckling safety of the carbon steel liner is also important and is sensitive to the method of the concrete dome placement, but is not treated here.

Ring beam

Primary purpose of the ring beam is to absorb a major portion of the thrust transmitted from roof dome thus reducing excessive deformation of the upper part of the wall. Therefore, dimensions of ring beam and the amount of prestressing tendons inside the ring beam have close relationship with the shape of roof dome. From the geometrical consideration, higher rise domes induce less thrust to the ring beam. Thus, a higher rise dome for above-ground LNG tanks to a certain extent is also beneficial for the ring beam as well as the dome itself. No tensile stress is intended to exist in the ring beam in the present design of LNG tank with 200,000 m^3 capacity.

Outer wall

Some important points in the design of the concrete tank wall are illustrated. LNG pressure is the main design loading of the outer wall, where LNG is assumed to be in contact with the outer wall due to leakage from the inner tank. Horizontal hoop tendons are installed to counteract the design loadings and also to introduce some residual compressive stress in hoop direction. Vertical tendons are additionally required to control the stresses induced by vertical moment. Safety check should be performed for the construction as well as the operation phase according to the proper codes. The most important problem is how to control the excessive moment and

corresponding tensile stress at the lower part of wall that result from the restraint of wall deformation by the rigid bottom slab.

Some strategies to control the excessive tensile stress are revisited and a recent study related to the optimal installation of tendons is introduced in the followings. Most of the above ground LNG tanks in Korea have the wall type where the lower half of the wall has a varying thickness and the upper half has a constant thickness.

Design of Inner Tank

Nine percent nickel steel is used for the inner tank because it has superior strength and toughness even at temperatures as low as -162^0C. Since the inner tank wall must be thicker at larger tank capacities, 9% Ni steel plates thicker than anything produced before were used to construct this tank. Thirty (30) mm thick plates that were used for 80,000 m^3 class tanks, 40 mm thick plates for the 140,000 m^3 tanks, and 50 mm thick plates for the 180,000 m^3 tanks are required. The strength and toughness were enhanced for the thick 9% Ni steel by introducing the latest technologies in steel production that helped to improve the heat treatment process and reduce impurities. In the process of commercializing thick 9% Ni steel, a number of strength and toughness tests were performed, including the low-temperature fracture tests, in order to ensure the material's safety for use in a large-capacity tank.

The objective of the present work is to design a robust LNG storage tank system which continues to function well when the future load, fluid, structural, material, and thermal properties are uncertain. The maximum thermal stress was evaluated by means of ALGOR---a FEA package which performs design analysis, simulation and optimization. The random variables for

maximum thermal stress considered are tabulated in Tables I. A probabilistic analysis was performed in order to include the uncertainty of the random variables in the design.

Table I. Random variables for thermal stress calculation

Random Variable	Mean Value
Temperature inside. T_i	-162°C
Pressure Inlet, P_i	689.48 kPa
Internal Diameter, D_i	42m
Outside ambient temperature, T_o	35°C
Outside Heat Transfer Coefficient, h_o	10 W/m^2· K
Inside Heat Transfer Coefficient, h_i	0.098 W/m^2· K
Emissivity Factor of the roof, ε_1	0.7
Emissivity Factor of the suspended deck, ε_2	0.8
Height, H	40.0m
Young's Modulus of inner tank base, E_{11}	2.01E11 N/m^2
Coefficient of Thermal Expansion of inner tank base, A_{11}	0.117E-05 1/K
Poisson's ratio of inner tank base, v_{11}	0.29
Thickness of inner tank base, T_{11}	50mm
Thermal Conductivity of inner tank base, K_{11}	46.26 W/m·K
Young's Modulus of inner tank wall, E_{12}	2.01E11 N/m^2
Coefficient of Thermal Expansion of inner tank wall, A_{12}	0.117E-05 1/K
Poisson's ratio of inner tank wall, v_{12}	0.29

Thickness of inner tank wall, T_{12}	50mm
Thermal Conductivity of inner tank wall, K_{12}	46.26 W/m·K
Young's Modulus of inner tank top, E_{13}	2.01E11 N/m^2
Coefficient of Thermal Expansion of inner tank top, A_{13}	0.117E-05 1/K
Poisson's ratio of inner tank top, v_{13}	0.29
Thickness of inner tank top, T_{13}	50mm
Thermal Conductivity of inner tank top, K_{13}	46.26 W/m·K
Young's Modulus of Insulation bottom, E_{21}	1.52E10 N/m^2
Coefficient of Thermal Expansion of Insulation bottom, A_{21}	3.600E-05 1/K
Poisson's ratio of Insulation bottom, v_{21}	0.3
Thickness of Insulation bottom, T_{21}	1200mm
Thermal Conductivity of Insulation bottom, K_{21}	0.052 W/m·K
Young's Modulus of Insulation wall, E_{22}	1.52E10 N/m^2
Coefficient of Thermal Expansion of Insulation wall, A_{22}	3.600E-05 1/K
Poisson's ratio of Insulation wall, v_{22}	0.3
Thickness of Insulation wall, T_{22}	1200mm
Thermal Conductivity of Insulation wall, K_{22}	0.052 W/m·K
Young's Modulus of Insulation deck, E_{23}	1.52E10 N/m^2
Coefficient of Thermal Expansion of Insulation deck, A_{23}	3.600E-05 1/K
Poisson's ratio of Insulation deck, v_{23}	0.3
Thickness of Insulation deck, T_{23}	400mm
Thermal Conductivity of Insulation deck, K_{23}	0.052 W/m·K

Young's Modulus of Bottom Base, E_{31}	$3.1E10 \text{ N/m}^2$
Coefficient of Thermal Expansion of Bottom Base, A_{31}	0.989E-05 1/K
Poisson's ratio of Bottom Base, v_{31}	0.15
Thickness of Bottom Base, T_{31}	2000mmn
Thermal Conductivity of Bottom Base, K_{31}	2.324 W/m·K
Young's Modulus of Outer Tank, E_{32}	$3.1E10 \text{ N/m}^2$
Coefficient of Thermal Expansion of Outer tank, A_{32}	0.989E-05 1/K
Poisson's ratio of outer tank, v_{32}	0.15
Thickness of outer tank, T_{32}	750mm
Thermal Conductivity of Outer Tank, K_{32}	2.324 W/m·K
Young's Modulus of Roof, E_{33}	$3.1E10 \text{ N/m}^2$
Coefficient of Thermal Expansion of Roof, A_{33}	0.989E-05 1/K
Poisson's ratio of Roof, v_{33}	0.15
Thickness of Roof, T_{33}	600mm
Thermal Conductivity of Roof, K_{33}	2.32 W/m·K

CHAPTER III

ANALYSIS

Finite Element Solution for Heat Transfer

Let us consider a two-dimensional partial differential equation of the form

$$\frac{1}{r}\frac{\partial}{\partial r}\left[rK_{rr}\frac{\partial T}{\partial r}\right] + \frac{\partial}{\partial z}\left[K_{zz}\frac{\partial T}{\partial z}\right] + PT + Q = 0 \text{ in A} \tag{1}$$

with the boundary conditions

$$T = T_0 \text{ on } L_1 \tag{2}$$

or

$$K_{rr}\frac{\partial T}{\partial r}n_r + K_{\theta\theta}\frac{\partial T}{\partial z}n_z + \alpha T + \beta = 0 \text{ on } L_2 \tag{3}$$

The corresponding functional is

$$I = \iint_A \left\{\frac{1}{2}K_{rr}\left(\frac{\partial T}{\partial r}\right)^2 + \frac{1}{2}K_{zz}\left(\frac{\partial T}{\partial z}\right)^2 - \frac{1}{2}PT^2 - QT\right\}2\pi r \ dA$$

$$+ \int_{L_2} \left(\frac{1}{2}\alpha T^2 + \beta T\right)2\pi r \ dL_2 \tag{4}$$

.

Here, n_r and n_z are direction cosines of the outward normal to L_2.

Simplex elements for this problem are axisymmetric rings whose properties are independent of the angle θ.

Element interpolation functions are taken as linear, of the form

$$T^{(e)} = N_i T_i + N_j T_j + N_k T_k \tag{5}$$

where the pyramid functions are

$$N_i = \frac{1}{2A}(a_i + b_i r + c_i z), \begin{cases} a_i = R_j Z_k - R_k Z_j \\ b_i = Z_j - Z_k \\ c_i = R_k - R_j \end{cases}$$

$$N_j = \frac{1}{2A}(a_j + b_j r + c_j z), \begin{cases} a_j = R_k Z_i - R_i Z_k \\ b_j = Z_k - Z_i \\ c_j = R_i - R_k \end{cases}$$

$$N_k = \frac{1}{2A}(a_k + b_k r + c_k z), \begin{cases} a_k = R_i Z_j - R_j Z_i \\ b_k = Z_i - Z_j \\ c_k = R_j - R_i \end{cases}$$

and $2A = b_i c_j + b_j c_i$ \hfill (6)

Here, R_i and Z_i denote the coordinates of the node i.

The element minimization equations are

$$\left\{ \begin{array}{c} \dfrac{\partial I}{\partial T_i} \\ \dfrac{\partial I}{\partial T_j} \\ \dfrac{\partial I}{\partial T_k} \end{array} \right\}^{(e)} = [B]^{(e)} \{T\}^{(e)} - \{C\}^{(e)} \qquad (7)$$

where the element matrix is

$$[B]^{(e)} = \iint_{A^{(e)}} (2\pi r) \left[[D]^T [K][D] - P\{N\}^T \{N\} \right] dA \\ + \int_{L^{(e)}} (2\pi r)\, \alpha\, \{N\}^T \{N\} dL_2 \qquad (8)$$

and the element column is

$$[C]^{(e)} = \iint_{A^{(e)}} (2\pi r)\, Q\, [N]^T\, dA \\ + \int_{L_2^{(e)}} (2\pi r)\, \beta\, \{N\}^T\, dL_2 \qquad (9)$$

These relations can now be evaluated for a simplex ring element.

In the case of the simplex element with a centroidal radial approximation, the radial term $2\pi\bar{r}$ simply comes outside of the element integrals. The result is

$$[B]^{(e)} = 2\pi\bar{r} \iint_{A^{(e)}} \left[[D]^T [K][D] - P\{N\}^T \{N\} \right] dA \\ + 2\pi\bar{r}_s \int_{L^{(e)}} \alpha\{N\}^T \{N\}\, dL_2 \qquad (10)$$

and

$$[C]^{(e)} = 2\pi\bar{r} \iint_{A^{(e)}} Q\, [N]^T\, dA \\ + 2\pi\bar{r}_s \int_{L_2^{(e)}} \beta\, \{N\}^T\, dL_2 \qquad (11)$$

17

Here r_s denotes the centroid of the side. The integrals that remain are the same as those in Cartesian coordinates.

For constant property elements, the element matrix becomes

$$[B]^{(e)} = \frac{2\pi\bar{r}K_{rr}}{4A}\begin{bmatrix} b_i b_i & b_i b_j & b_i b_k \\ b_i b_j & b_j b_j & b_j b_k \\ b_i b_k & b_j b_k & b_k b_k \end{bmatrix}^{(e)} \qquad (K_{ss} \text{ matrix})$$

$$+ \frac{2\pi\bar{r}K_{rr}}{4A}\begin{bmatrix} c_i c_i & c_i c_j & c_i c_k \\ c_i c_j & c_j c_j & c_j c_k \\ c_i c_k & c_j c_k & c_k c_k \end{bmatrix}^{(e)} \qquad (K_{zz} \text{ matrix})$$

$$- \frac{2\pi \ \bar{r} \ PA}{12}\begin{bmatrix} 2 & 1 & 1 \\ 1 & 2 & 1 \\ 1 & 1 & 2 \end{bmatrix}^{(e)} \qquad (P \text{ matrix})$$

$$+ \frac{2\pi}{6}(\alpha\bar{r}L)_{ij}\begin{bmatrix} 2 & 1 & 0 \\ 1 & 2 & 0 \\ 0 & 0 & 0 \end{bmatrix}^{(e)}_{\text{on side ij}} \qquad (\alpha \text{ matrix } ij)$$

$$+ \frac{2\pi}{6}(\alpha\bar{r}L)_{jk}\begin{bmatrix} 0 & 0 & 0 \\ 0 & 2 & 1 \\ 0 & 1 & 2 \end{bmatrix}^{(e)}_{\text{on side jk}} \qquad (\alpha \text{ matrix } jk)$$

18

$$
+\frac{2\pi}{6}(\alpha\bar{r}L)_{ki}\begin{bmatrix} 2 & 0 & 1 \\ 0 & 0 & 0 \\ 1 & 0 & 2 \end{bmatrix}^{(e)}_{\text{on side } ki} \qquad\qquad (\alpha \text{ matrix } ki)
$$

$$(12)$$

and the element column is

$$
\{C\}^{(e)} = \frac{2\pi\bar{r}QA}{3}\begin{Bmatrix} 1 \\ 1 \\ 1 \end{Bmatrix}^{(e)} \qquad\qquad (Q \text{ column})
$$

$$
-\frac{2\pi(\beta\bar{r}L)_{ij}}{2}\begin{Bmatrix} 1 \\ 1 \\ 0 \end{Bmatrix}^{(e)} \qquad\qquad (\beta \text{ column } ij)
$$

$$
-\frac{2\pi(\beta\bar{r}L)_{jk}}{2}\begin{Bmatrix} 0 \\ 1 \\ 1 \end{Bmatrix}^{(e)} \qquad\qquad (\beta \text{ column } jk)
$$

$$
-\frac{2\pi(\beta\bar{r}L)_{ki}}{2}\begin{Bmatrix} 1 \\ 0 \\ 1 \end{Bmatrix}^{(e)} \qquad\qquad (\beta \text{ column } ki)
$$

$$(13)$$

On each side, the term $\bar{r}$ denotes the centroid of that side. As in the normal two-dimensional problem, the element matrix $[B]$ is a three by three matrix, and the element column $\{C\}$ is a three

component column. The element numbering (as given in the element/nodal connectivity data) must be counterclockwise.

For the terms evaluated along the side of elements, β is taken to be constant within the element. The other quantities that must be found are the side lengths. They are given by

$$L_{ij} = \left[\left(R_i - R_j \right)^2 + \left(Z_i - Z_j \right)^2 \right]^{1/2}$$

$$L_{jk} = \left[\left(R_j - R_k \right)^2 + \left(Z_j - Z_k \right)^2 \right]^{1/2}$$

$$L_{ki} = \left[\left(R_k - R_i \right)^2 + \left(Z_k - Z_k \right)^2 \right]^{1/2} \qquad (14)$$

Only if the derivative boundary conditions are to be imposed on a certain side are the derivative boundary matrix and column included in the appropriate element matrix and column.

The element matrices were then assembled into the global matrices and vectors. The prescribed boundary conditions were implemented at the appropriate nodal points. The algebraic equations in the global assembled form were solved by the Gauss elimination procedure. These details are not shown in order to conserve space.

Procedure for Thermal Stress Evaluation

If the distribution of the change in temperature $\Delta T(x, y)$ is known, the strain

due to this change in temperature can be treated as an initial strain ε_0. From

the theory of mechanics of solids, ε_0 for plane stress can be represented by

$$\varepsilon_0 = (\alpha\Delta T, \alpha\Delta T, 0)^T \tag{15}$$

and the plane strain is given by

$$\varepsilon_0 = (1 + \nu)(\alpha\Delta T, \alpha\Delta T, 0)^T \tag{16}$$

The stresses and strains are related by

$$\sigma = D(\varepsilon - \varepsilon_0) \tag{17}$$

Where D is the symmetric (6 X6) material matrix given by

$$D = \frac{E}{(1+\nu)(1-2\nu)}\begin{bmatrix} 1-\nu & \nu & \nu & 0 & 0 & 0 \\ \nu & 1-\nu & \nu & 0 & 0 & 0 \\ \nu & \nu & 1-\nu & 0 & 0 & 0 \\ 0 & 0 & 0 & 0.5-\nu & 0 & 0 \\ 0 & 0 & 0 & 0.5-\nu & 0 & 0 \\ 0 & 0 & 0 & 0 & 0 & 0.5-\nu \end{bmatrix} \tag{18}$$

The effect of temperature can be accounted for by considering the strain

energy term.

$$U = \frac{1}{2}\int (\varepsilon - \varepsilon_0)^T D(\varepsilon - \varepsilon_0) t dA$$

$$= \frac{1}{2}\int (\varepsilon^T D\varepsilon - 2\varepsilon^T D\varepsilon_0 + \varepsilon_0^T D\varepsilon_0) t dA \tag{19}$$

The first term in the previous expansion gives the stiffness matrix derived earlier. The last term is a constant, which has no effect on the minimization process. The middle term, which yields the temperature load, is now considered in detail. Using the strain-displacement relationship $\varepsilon = Bq$,

$$\int_A \varepsilon^T D\varepsilon_0 t dA = \sum_e q^T (B^T D\varepsilon_0) t_e A_e \tag{20}$$

This step is obtained using the Galerkin approach where ε^T will be $\varepsilon^T(\phi)$ and q^T will be ψ^T. The symbol ϕ defines the shape function and ψ defines the weight function. It is convenient to designate the element temperature load as

$$\theta^e = t_e A_e B^T D\varepsilon_0 \tag{21}$$

Where,

$$\theta^e = [\theta_1, \theta_2, \theta_3, \theta_4, \theta_5, \theta_6]^T \tag{22}$$

The vector ε_0 is the strain in Equation (1) due to the average temperature change in the element. θ^e represents the element nodal load distributions that must be added to the global force vector.

The stresses in an element are then obtained by using Equation (3) in the form

$$\sigma = D(Bq - \varepsilon_0) \tag{23}$$

Linear Steady-State Heat Transfer Analysis

Linear steady-state heat transfer occurs when the material's conductivity is not dependent on temperature. But in our case, the properties of outer tank are dependent on temperature. Nonlinear heat transfer analysis is considered in this thesis.

Fourier's law of heat conduction is given by $Q = -kA \nabla T$

- Q = heat flow
- k = thermal conductivity (a constant) entered as a material property. Isotropic materials fall under this category.
- A = cross sectional area of an element face
- ∇T= the temperature gradient in the direction normal to the area, A

The convection is given by $Q = hA\Delta T$

- h = convective heat-transfer coefficient (constant) entered by the user.
- A = area of the element subject to convection
- $\Delta T = T_s - T$
- T_s = surface temperature of the element (calculated)
- T = temperature of the fluid (assumed to be constant) and entered by the user.

The heat flux (heat transfer/time/area) experienced by a surface subjected to thermal radiation is described by the following equations:

$$q'' = F_{rad} \sigma (T_s{}^4 - T_{rad}{}^4)$$

- q'' = thermal radiative heat flux
- F_{rad} = radiation view factor, which includes absorptivity, emissivity and view factor effects
- σ = Stefan-Boltzmann constant

- T_s = calculated surface temperature on an absolute scale

- T_{rad} = ambient temperature

Due to the higher outside ambient temperature relative to that of the cryogenic liquid, heat is always being transferred to the cryogenic liquid. The bottom layer of the LNG tank is always at the higher temperature than the top layer of LNG. A buoyancy force is generated in the fluid when it is heated or cooled by a surface. Since hot LNG is less dense than the cold LNG, natural convection occurs due to differences in density. This causes motion in the fluid as the warm fluid rises and the cool fluid is then moved to the surface where it will be heated.

The Rayleigh number for a fluid is a dimensionless number associated with buoyancy driven flow in an enclosure. When the Rayleigh number is below a certain critical value for a fluid heat transfer in the fluid is primarily by conduction and by convection when it exceeds this value. The Nusselt number is given by $0.13*Ra^{1/3}$ where Ra is the Rayleigh number [16]. The Rayleigh number is assumed to be 10^6 since the diameter and height of the tank is dozens of meters [16]. From the Nusselt number, the inside convective heat transfer coefficient is calculated to be 0.098W/m2 K. The outside heat transfer coefficient in the present work is taken to be 10W/(m2·K) which is a typical value for an experimentally determined ambient convection coefficient on a vertical surface.

FEA Analysis Procedure

The sketch mode in ALGOR was used to build the axisymmetric LNG tank. In ALGOR 2D and axisymmetric models need to be built in the YZ plane. After the outline of the tank is created, the 'mesh between the object groups' command is used to create the mesh. The mesh

needs to maintain the connectivity between the nodes (otherwise there will be no transfer of loads from one node to another). Once the geometry is ready, the correct element type (axisymmetric) and the material properties were assigned.

In this study, the heat transfer analysis was performed first in ALGOR to use the results in later analyses. Since ALGOR cannot perform heat transfer and static stress simultaneously, the heat transfer analysis was performed first and then the results of the thermal analysis were imported to the static stress analysis. In order to calculate maximum boil-off, only the steady-state heat transfer analysis is required. To calculate thermal stresses, however, the steady-state heat transfer analysis was performed first and then the static stress analysis was performed since the stresses depend on the temperature field as well as the mechanical loading.

All the boundary conditions and the loads are applied to the model and the steady state thermal analysis is performed. ALGOR creates a ".to" file in which temperature at each nodal point is saved during this analysis. From the results of this file, the maximum temperature is noted. To calculate boil-off only, the heat rate transferring through the face of the element is calculated and summed up for all the elements to obtain the heat gained by the LNG.

Once the temperature results are calculated, the mode of the analysis is changed from steady-state heat transfer to linear static stress. The results from the heat transfer were then imported to this linear static analysis by going into the analysis parameter command and picking the corresponding file. Von Mises stresses are calculated at each node by ALGOR. From these nodal values, the maximum von Mises stress can be found.

In this thesis, we are considering 54 random variables for the linear static stress analysis. In every run, one variable is changed by +/- 10% while keeping the others unchanged and each time the analysis is run a new von Mises stress is recorded. The process is repeated until all the variables have been changed +/- 10%. One hundred and nine such runs are performed for all the variables to be changed by +/- 10%.

The stress results are entered into a probabilistic analysis program, NESTEM, wherein the probabilistic analysis is performed and the sensitivity factors for each random variable are determined.

Probabilistic Analysis:

The ability to quantify the uncertainty of complex engineered systems subject to inherent randomness in loading, environment, material properties, and geometric parameters is becoming increasingly important in design and certification efforts. Traditional design approaches typically use worst case assumptions and safety factors to certify a design. This approach is overly conservative, does not quantify the reliability; nor does it identify critical parameters or failure modes affecting the system performance.

A probabilistic analysis approach characterizes input variability using probability density functions and then propagates these density functions through the performance model to yield uncertain model outputs, which can be related to failure metrics such as fatigue life, rupture, or stress intensity. The approach quantifies the reliability, can reduce over-conservatism, and identifies critical parameters and failure modes driving the reliability of the system.

The programmers and researchers try to achieve the following in the development of the analysis algorithm.

- Identifying sources of errors and uncertainties

- Developing probability distributions for input variables

- Determining spatial and temporal variations

- Developing probabilistic load modeling

- Tailoring failure models for modeling uncertainty and obtaining appropriate system performance measure

- Creating system models (multiple failure mode and components)

NESTEM enables designers to achieve reliable and optimum designs subjected to a life constraint with a probabilistic treatment of key uncertainties. The NESTEM code has been under development at the NASA Glenn Research Center for over 15 years. NESTEM uses deterministic analyses together with probabilistic methods to quantify the probability of failure of structural components which are subjected to complex mechanical and thermal loading. The NESTEM code was developed to perform probabilistic analyses of structures subjected to either steady state or random thermal and mechanical loads. Probabilistic methods are becoming more and more useful due to the salient features of consistency, reliability and economy.

NESTEM is a modular computer software system for performing probabilistic analysis of structural/mechanical components and systems. NESTEM combines state-of-the-art probabilistic algorithms with general-purpose numerical analysis methods to compute the probabilistic response and reliability of engineered systems. Uncertainties in loading, material properties, geometry, boundary conditions and initial conditions can be simulated. Many deterministic modeling tools can be used such as finite elements, boundary elements, hydrocodes, and user-defined Fortran subroutines. NESTEM offers a wide range of capabilities, a graphical user interface, and is verified using hundreds of test problems.

NESTEM was initially developed by Southwest Research Institute (SwRI) for NASA to perform probabilistic analysis of space shuttle main engine components [17]. SwRI continues to develop and apply NESTEM to a diverse range of problems including aerospace structures, automotive structures, biomechanics, gas turbine engines, geomechanics, nuclear waste packaging, offshore structures, pipelines, and rotordynamics. To accomplish this, the codes have been interfaced with many well-known third-party and commercial deterministic analysis programs

CHAPTER IV

RESULTS AND DISCUSSION

The problem is solved iteratively by using a scattered set of values obtained by varying the mean variables by of the LNG storage tank +/- 10%. In the current work, a probabilistic analysis has been performed for the maximum von Mises stress. As shown in Figure 3, the model is created in ALGOR sketch mode and then carefully meshed. The outside ambient temperature boundary condition is set to 35°C degrees and the inside LNG temperature is set to -162°C degrees. The inlet pressure of the tank is set to 689.48kPa. The tank is fixed at the bottom base. All the random variables are assumed to be independent and a normal distribution is assumed for all random variables.

The maximum stress location is determined in the mean run and this location is used to evaluate the cumulative distribution functions and the stresses produced in LNG tank. A typical von Mises thermal stress distribution is shown in Figure 4 and Figure 5 depicts the temperature profile in the tank for the mean random variables. The probabilistic stress analysis is performed at the point of maximum stress which occurs at the bottom of the tank near the outer edge.
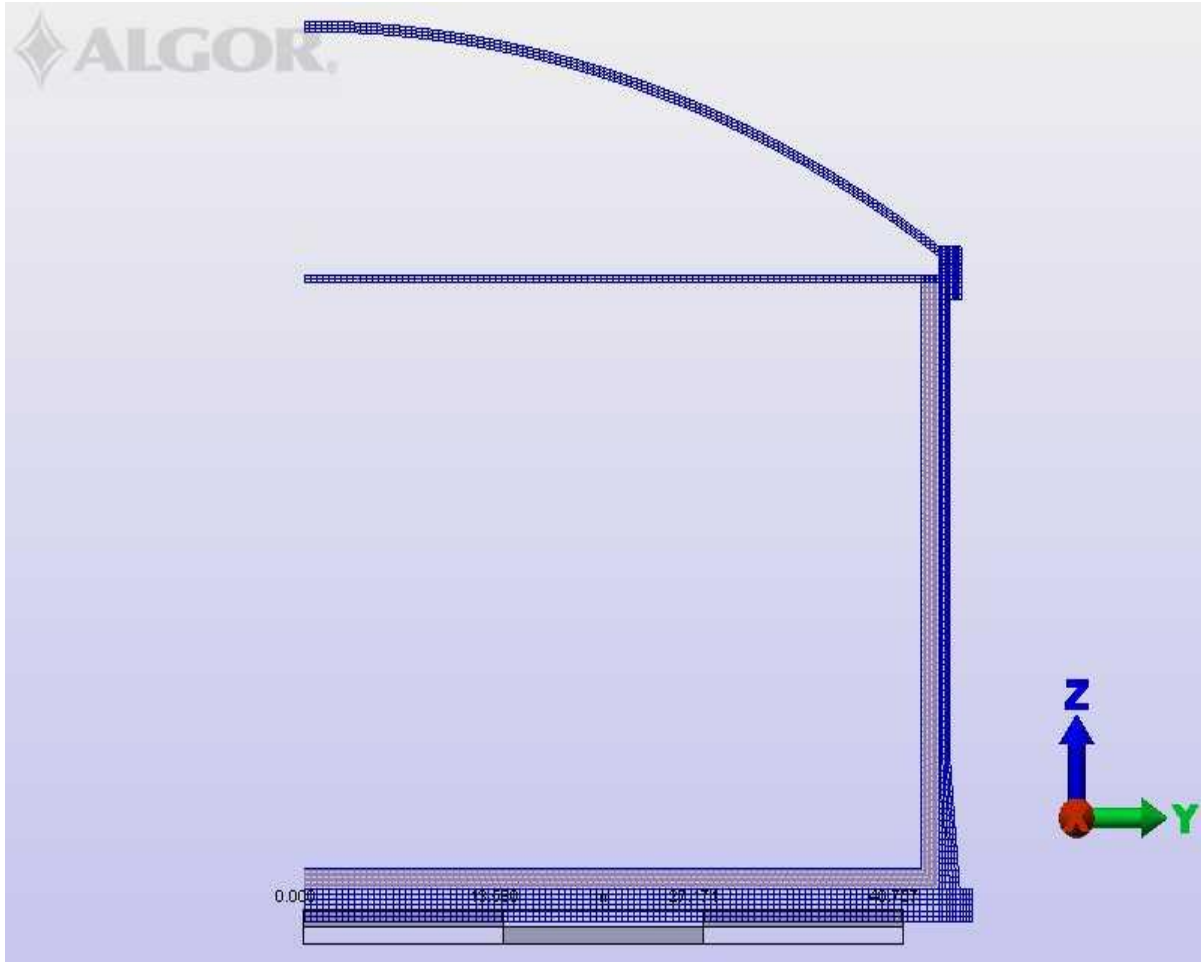
Figure 3. Meshed model of tank.
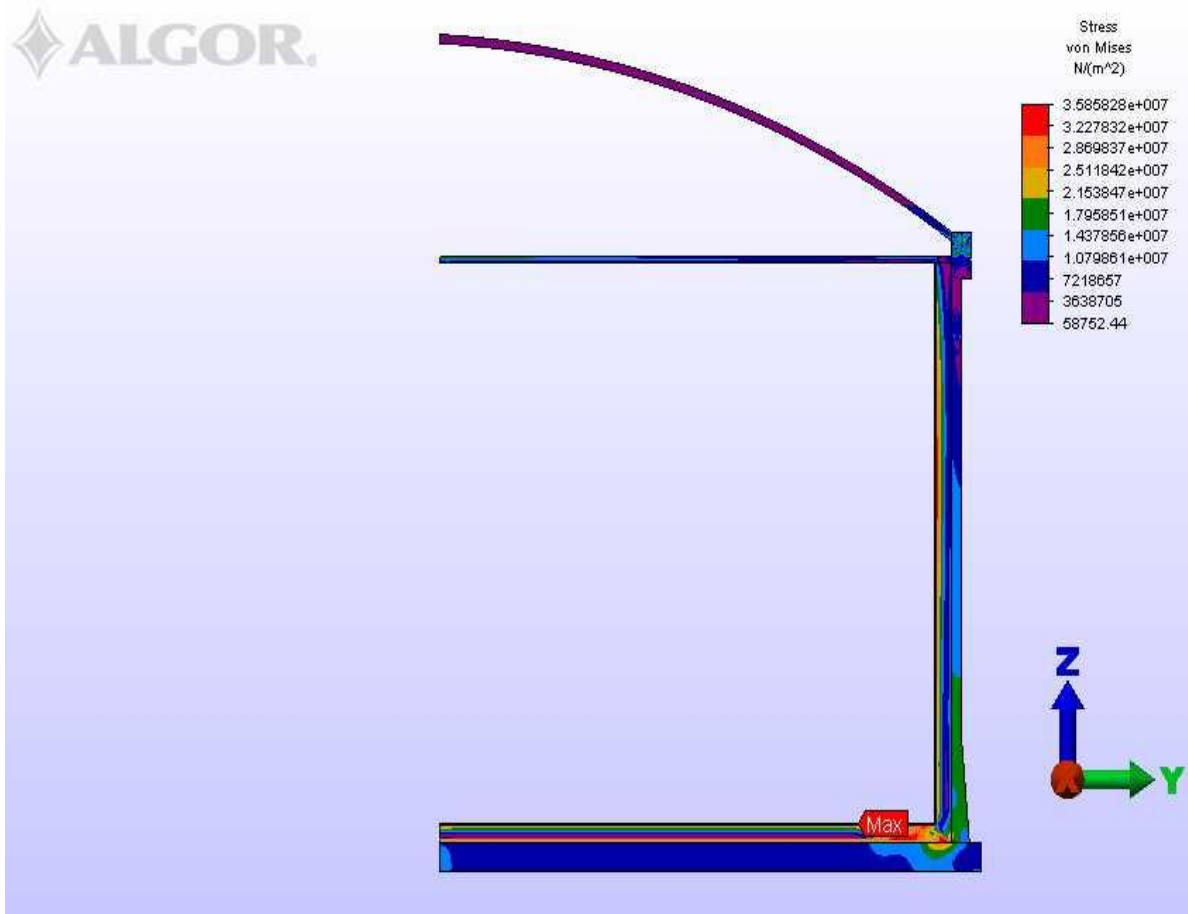
Figure 4. Thermal stress analysis of tank.
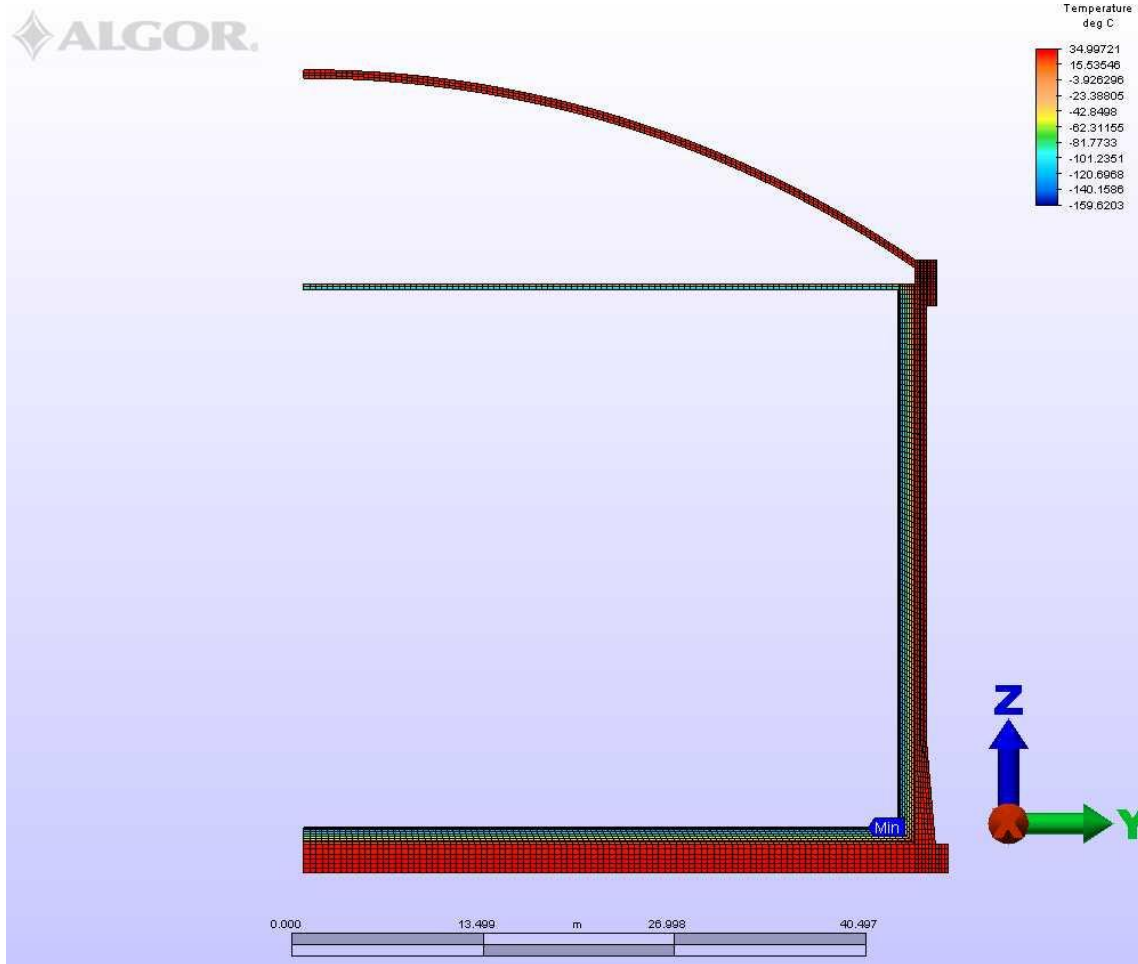
Figure 5. Temperature profile in tank.

FEA Results

Figures 6 to 16 show the sensitivity factors for stress for each random variable obtained from NESTEM and are plotted for each probability value from 0.001 to 0.999. Only twenty five of the 54 variables that influence stress the most are presented in these figures. For the variables number 7 to number 25 counting from left to right a special notation was used to specify if the random variable name refers to the bottom or the side of the tank. The random variable name with a "1" after it (for example "thickness of insulation1") means that it refers to the side of the tank whereas if there is no number after the random variable name it refers to bottom of the tank. No variables pertaining to the top or roof are presented in the figures since they do not

32

significantly contribute to the stress. For the first six random variable names, however: inner temperature to height of tank inclusive, the variable refers to both the side and the bottom of the tank. Figure 17 shows the cumulative probability of stress. The raw data obtained from the NESTEM analysis is also shown for the stress analysis.

The cumulative probabilities of stress in Figure 17 show the range of probability value from 0.001 to 0.999. The 50 percent probability represents the stress produced for the case when all of 54 variables are at the mean value which is the deterministic case. The stress at the 0.001 probability level is 2.97×10^8 N/m^2 and at the 0.999 probability level is 6.90×10^8 N/m^2.

Based on Figures 6 to 16, the inner temperature has the most influence on stress. The modulus of elasticity of bottom and side of inner tank, coefficients of expansion of the side and bottom of the inner tank, Poisson's ratio of the bottom of inner tank, thermal conductivity of insulation, and inside convection coefficient also influence the maximum stress. The somewhat arbitrary choice of the outside convection coefficient (10 W/m^2) can be justified in terms of the small influence it has on stress. Also the outside temperature choice can be justified in that it has a small bar in the sensitivity factor graphs.

Boil-off Calculation

The method of calculating the maximum quantity of boil-off gas generated is given. The total heat input to the LNG tank is the sum of the heat input to the roof, sides and bottom and is given by:

$Q_T = 249917$ J/sec

where

Q_T: total rate of heat input (J/sec)

The quantity of boil-off gas is calculated by

$q = Q_T / h_{fg}$

where

q: quantity of boil-off gas (kg/sec)

Q_T: total heat input (J/day)

h_{fg}: latent heat of vaporization (J/kg)

$q = 249917 / 506169 = 0.4937$ kg/sec

The maximum boil-off of gas in weight percent per day is given by

R = 24 (h/day) * 3600 (sec/h) * 100 q / m

R = 24*3600*100*0.4937 kg/sec/ 84589272 kg

R = 0.051% wt/day

where

R: maximum boil off gas rate in percent (wt/day)

m: mass of LNG (kg)

q: quantity of boil off gas (kg/sec)

Yang [8] examines a similar size tank to the one in this thesis--200000 m^3.

Yang gives a design boil off per day of 0.05% wt/day which is close to the boil off found in this

study which is 0.051% wt/day.
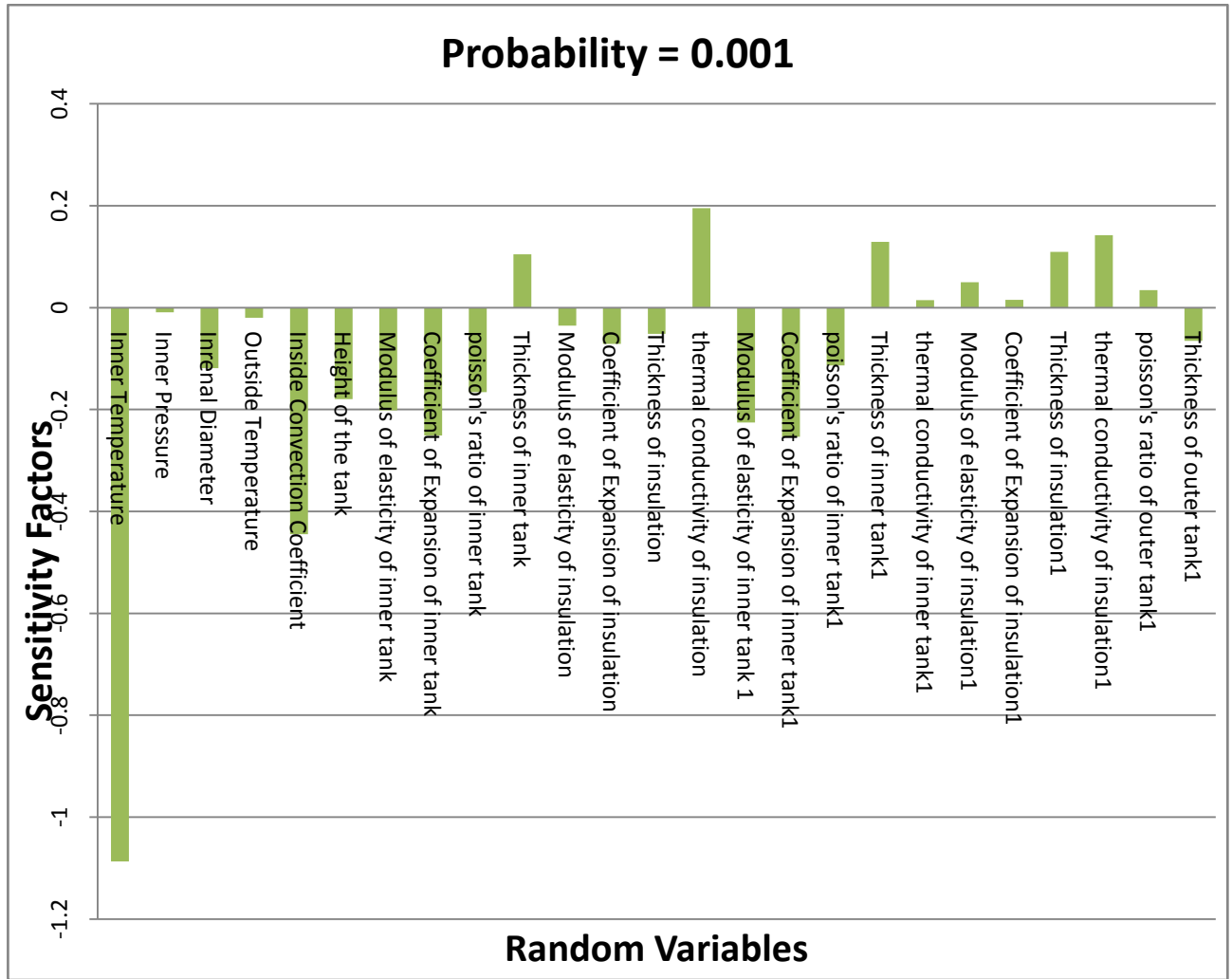
Figure 6. Sensitivity factor versus random variables for probability = 0.001.
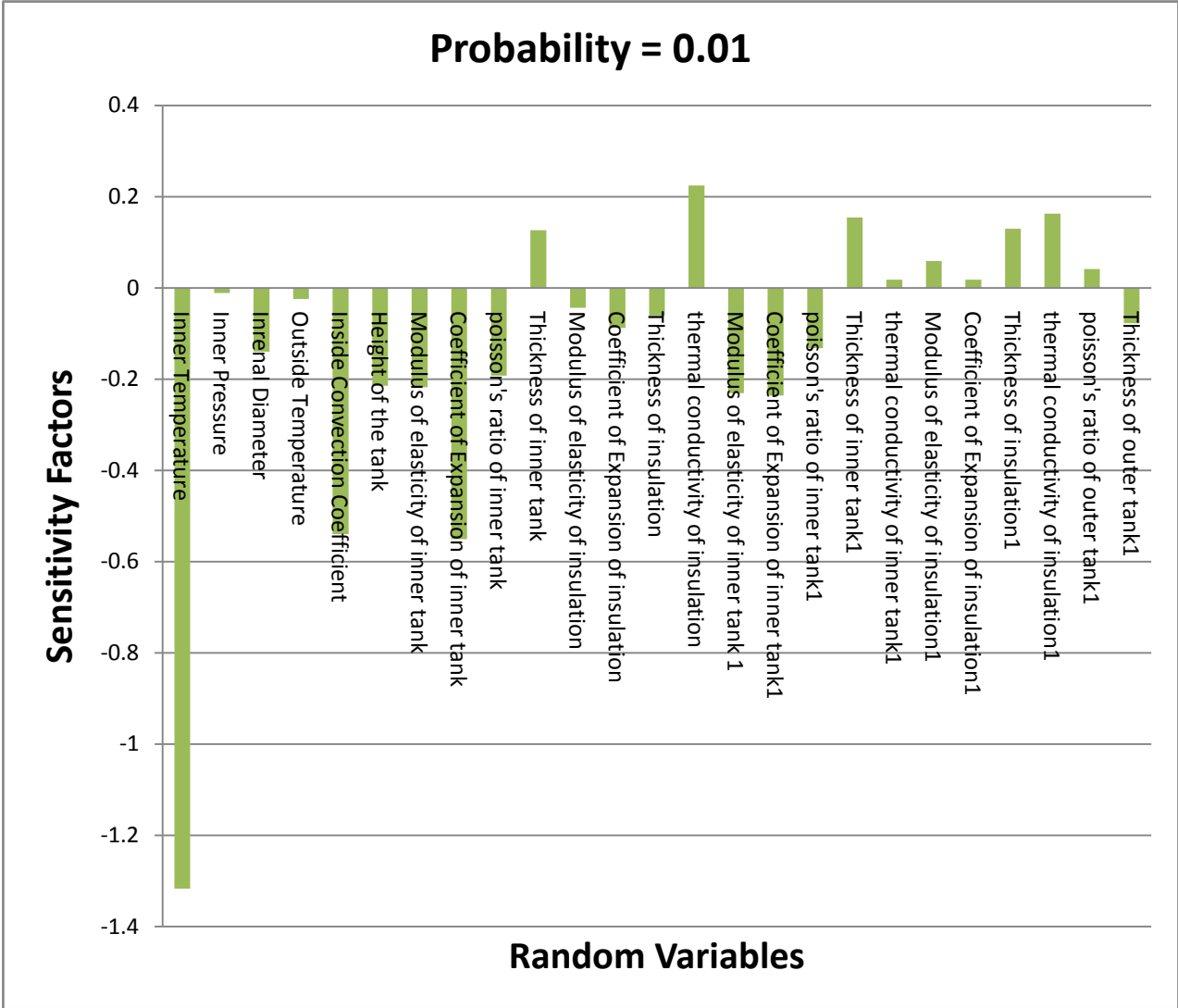
Figure 7. Sensitivity factor versus random variables for probability = 0.01.
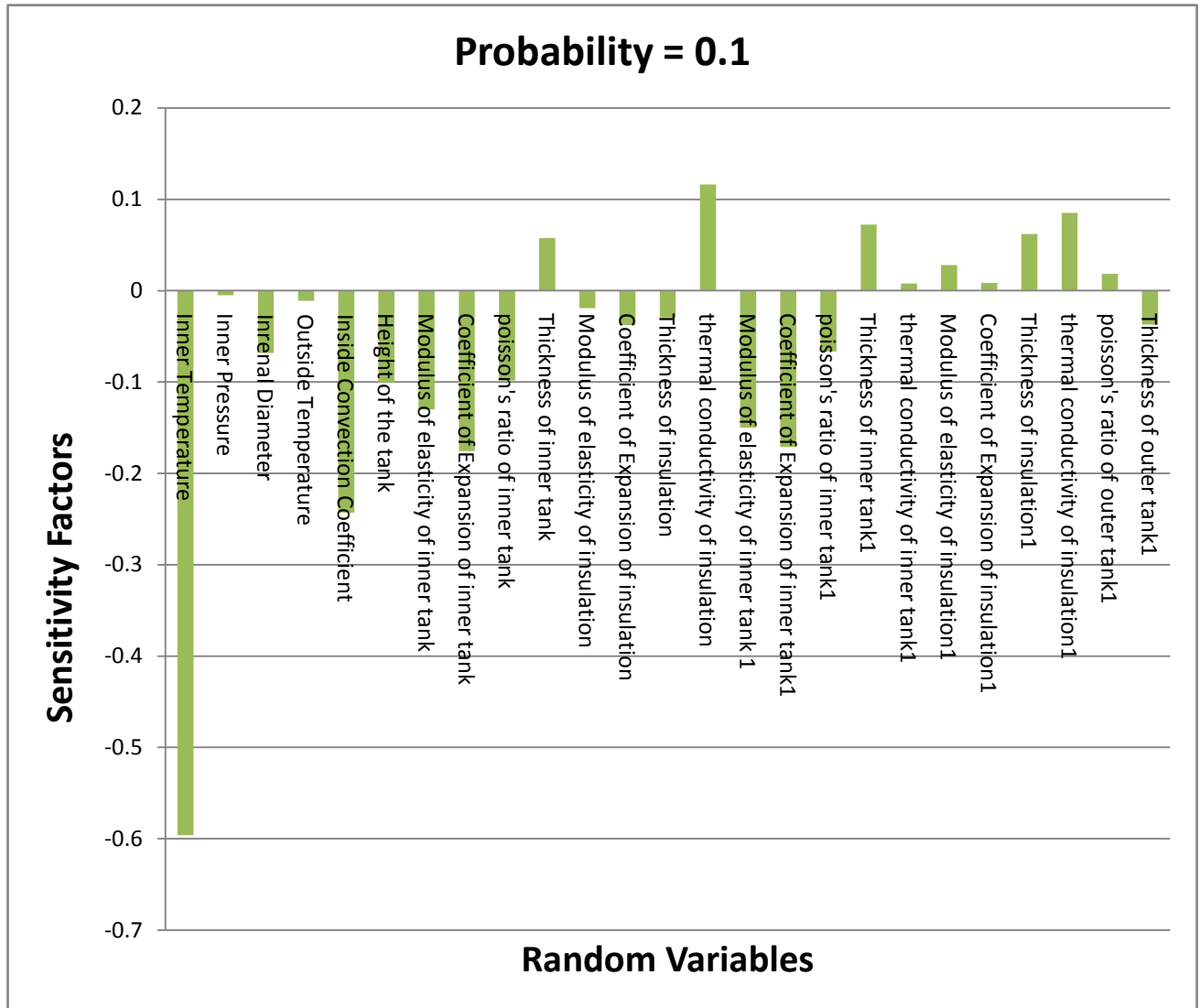
Figure 8. Sensitivity factor versus random variables for probability = 0.1.
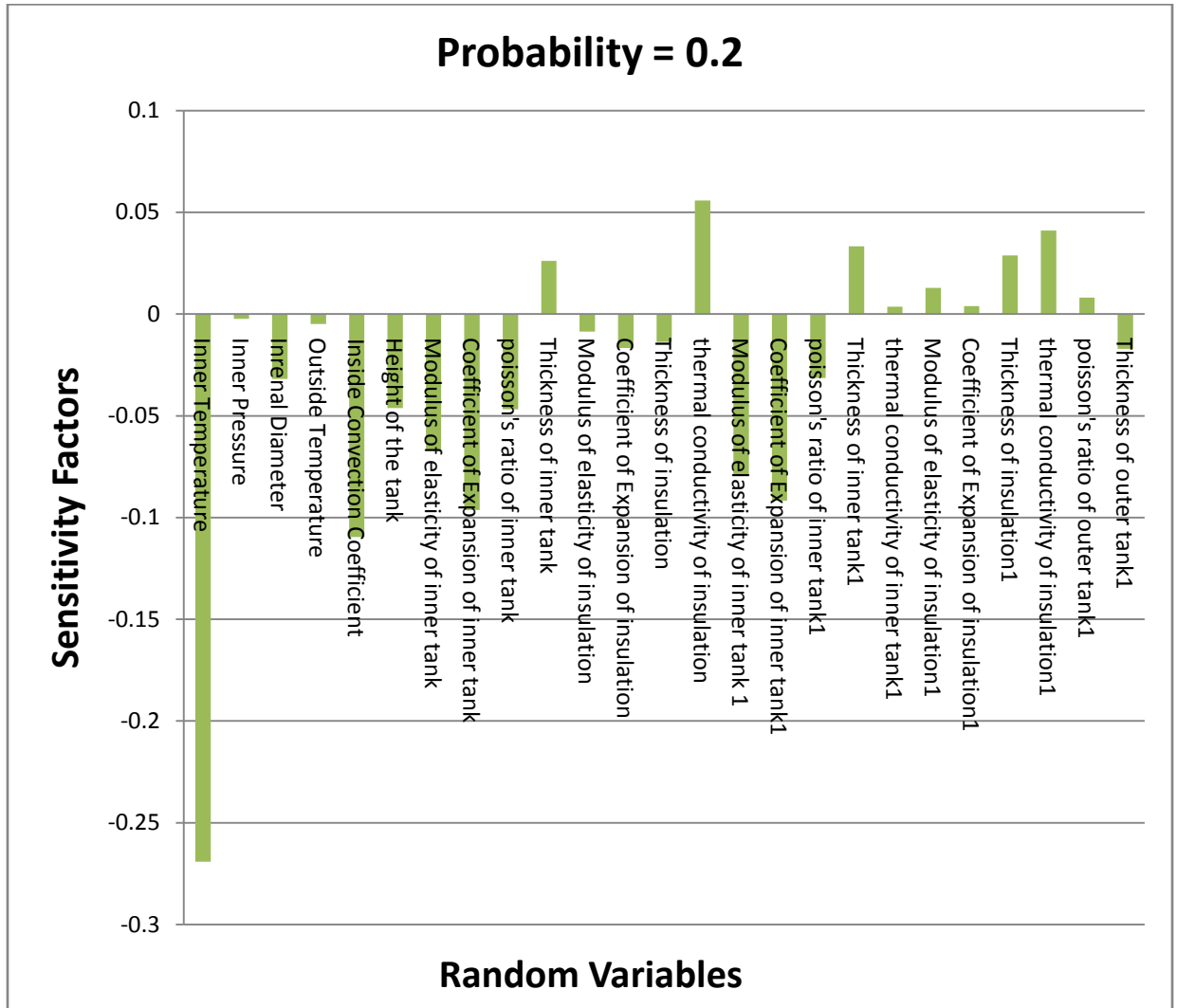
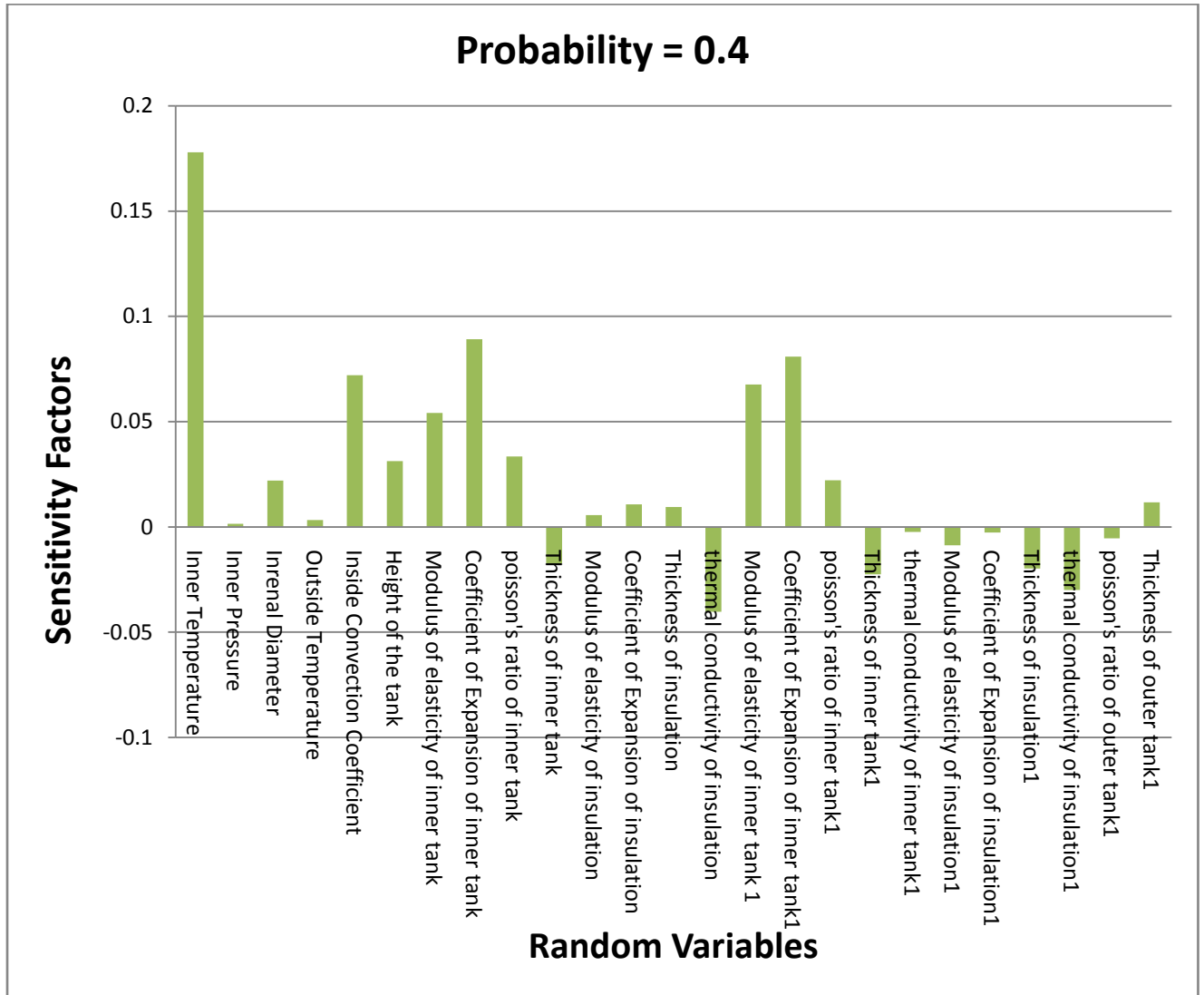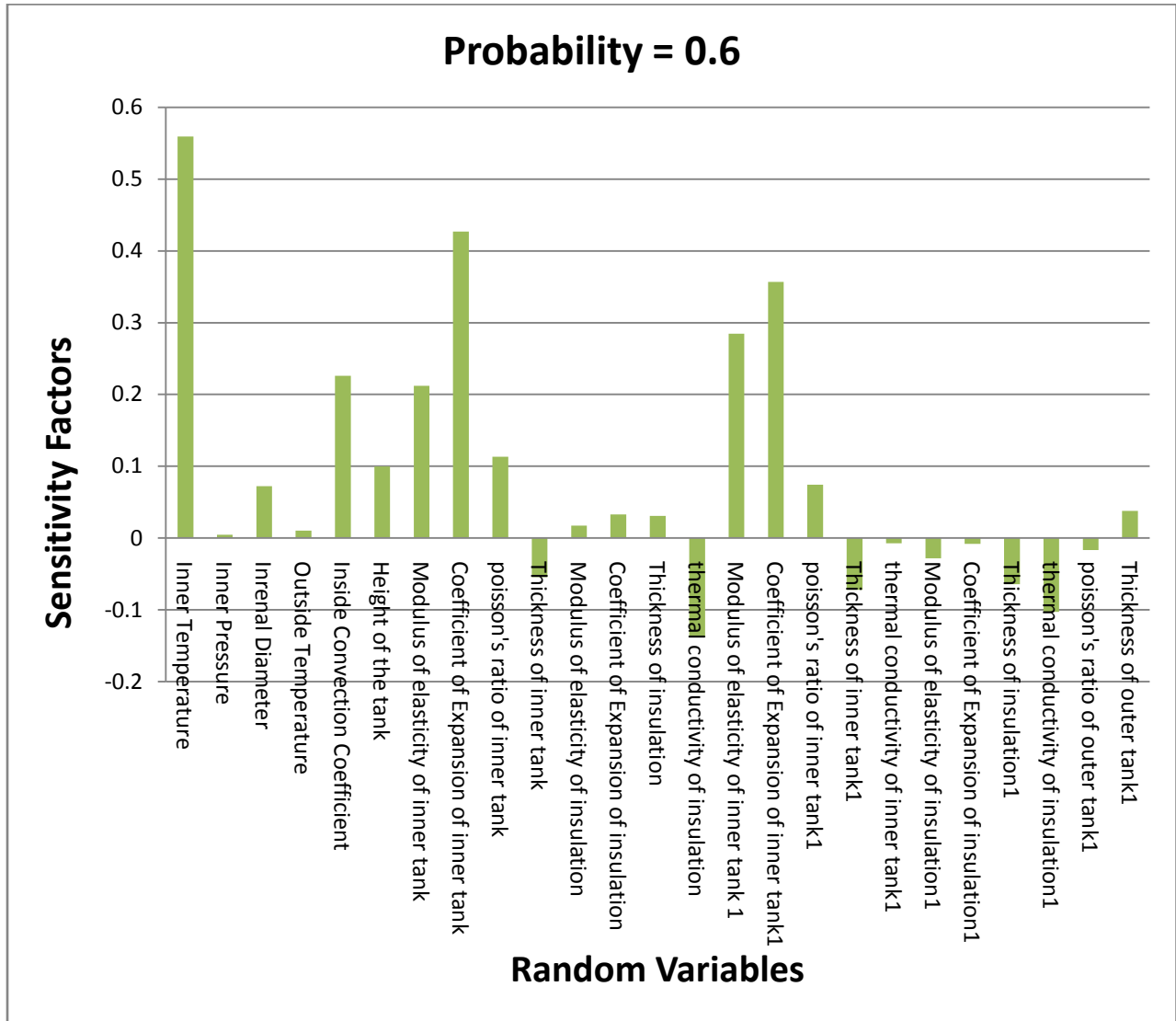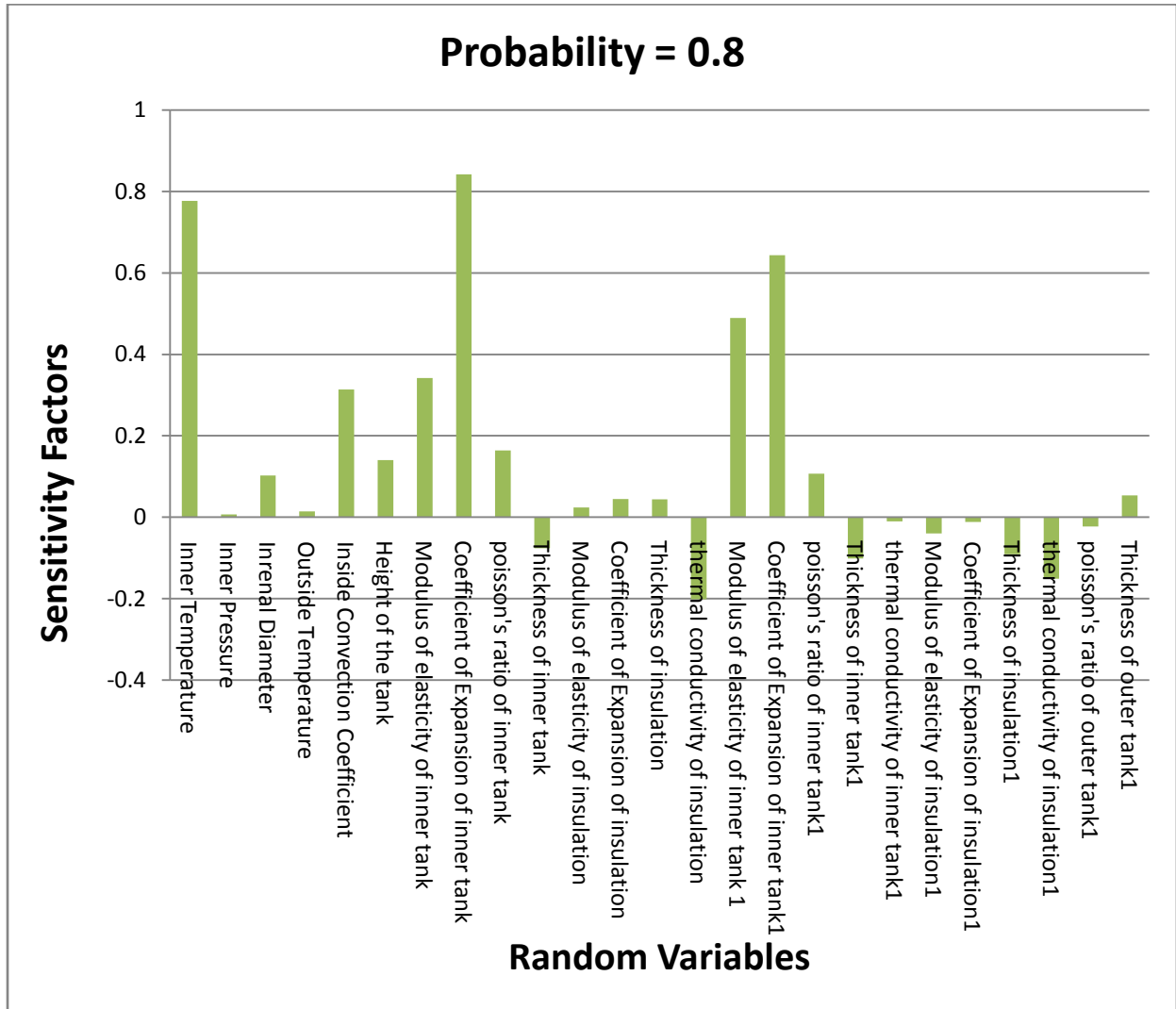Figure 9. Sensitivity factor versus random variables for probability = 0.2.

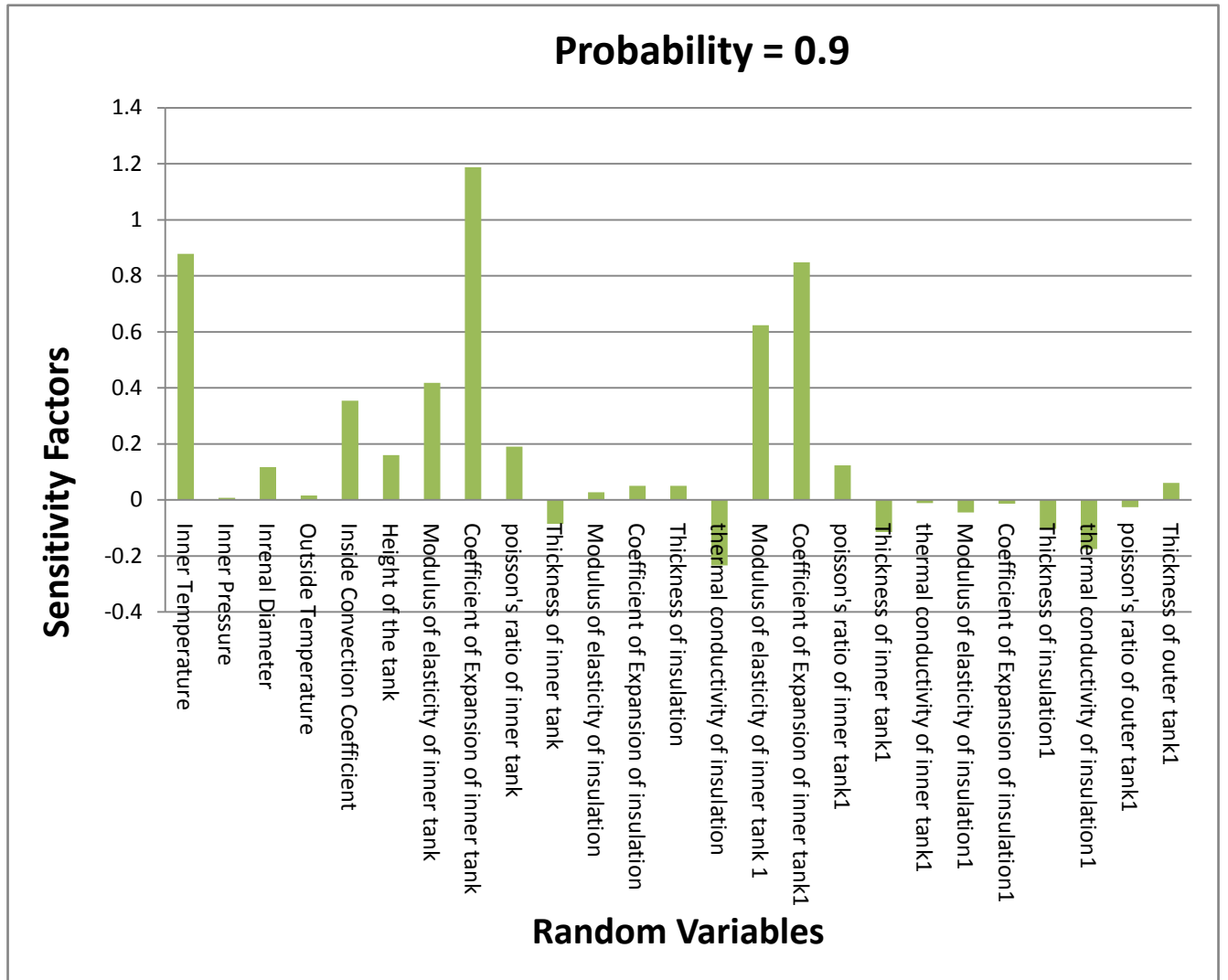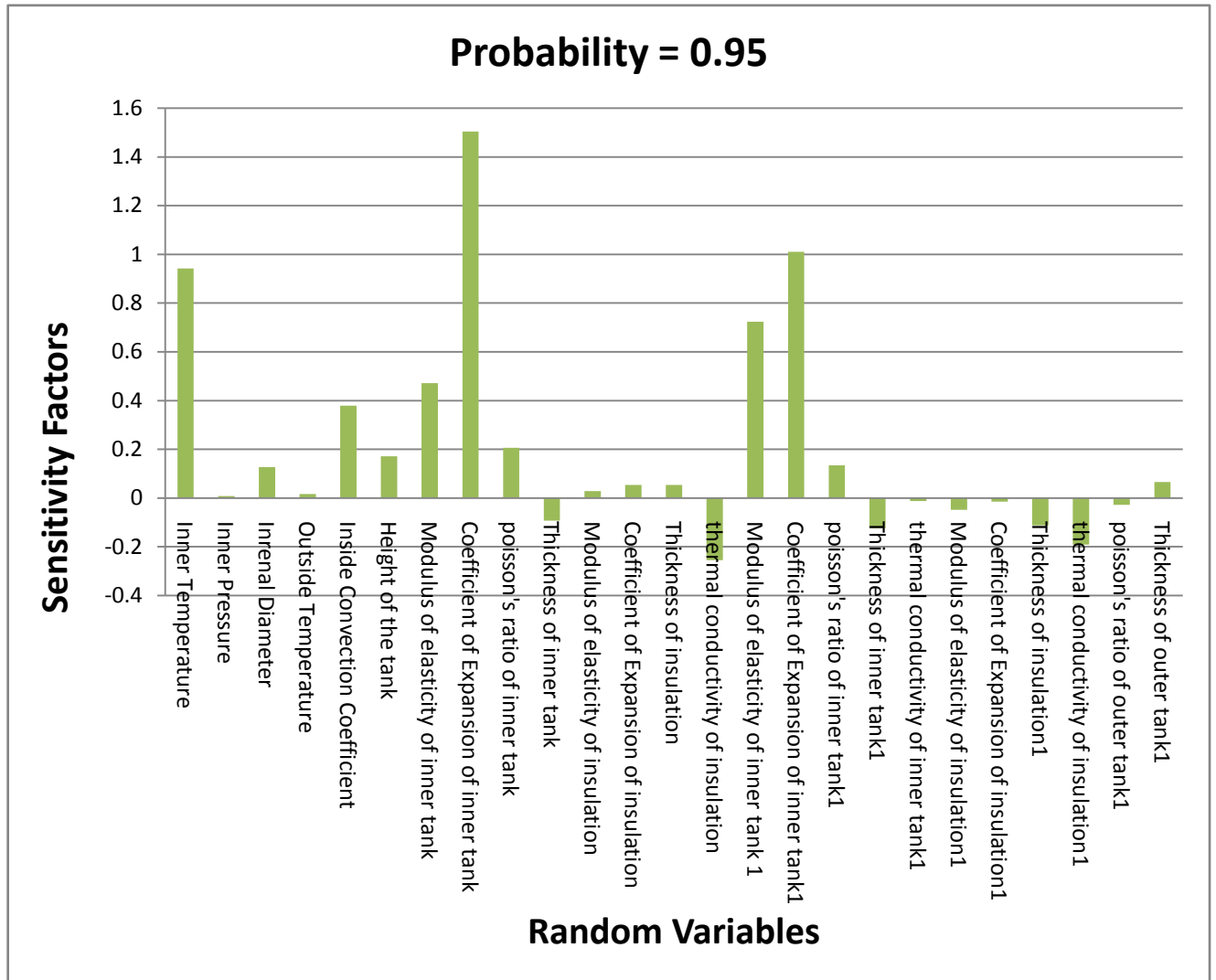Figure 10. Sensitivity factor versus random variables for probability = 0.4.

Figure 11. Sensitivity factor versus random variables for probability = 0.6.

Figure 12. Sensitivity factor versus random variables for probability = 0.8.

Figure 13. Sensitivity factor versus random variables for probability = 0.9.

Figure 14. Sensitivity factor versus random variables for probability = 0.95.
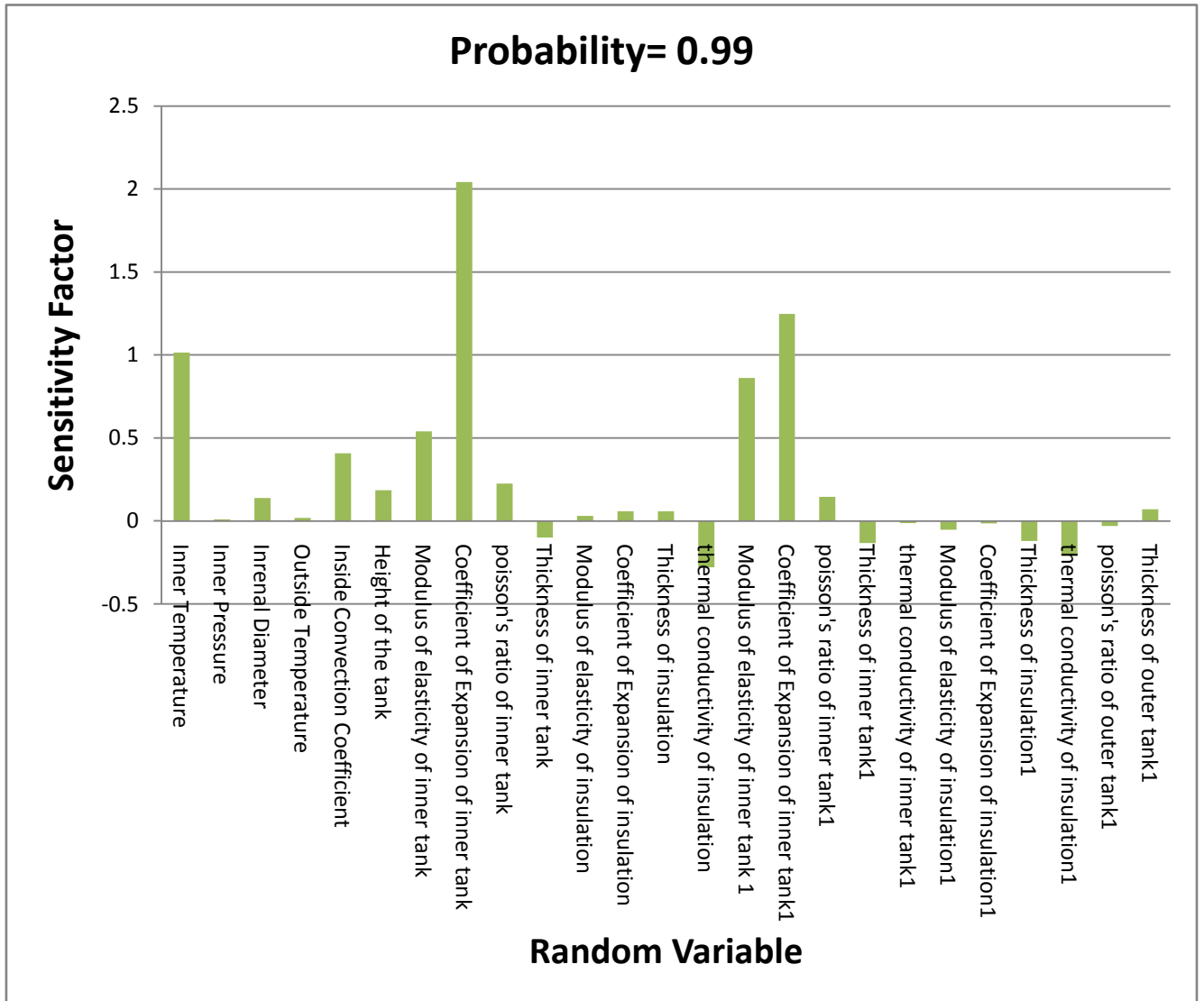
Figure 15. Sensitivity factor versus random variables for probability = 0.99.
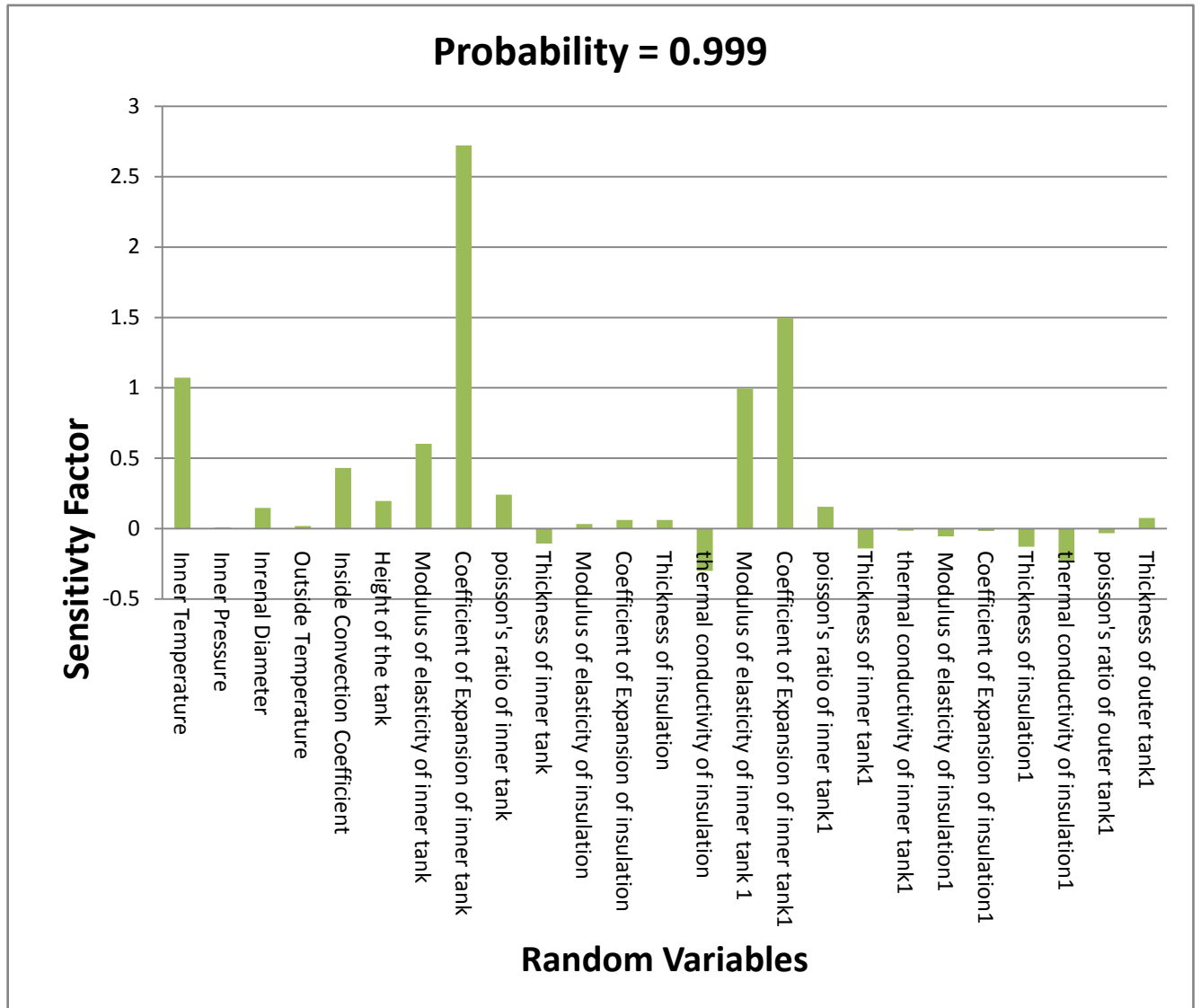
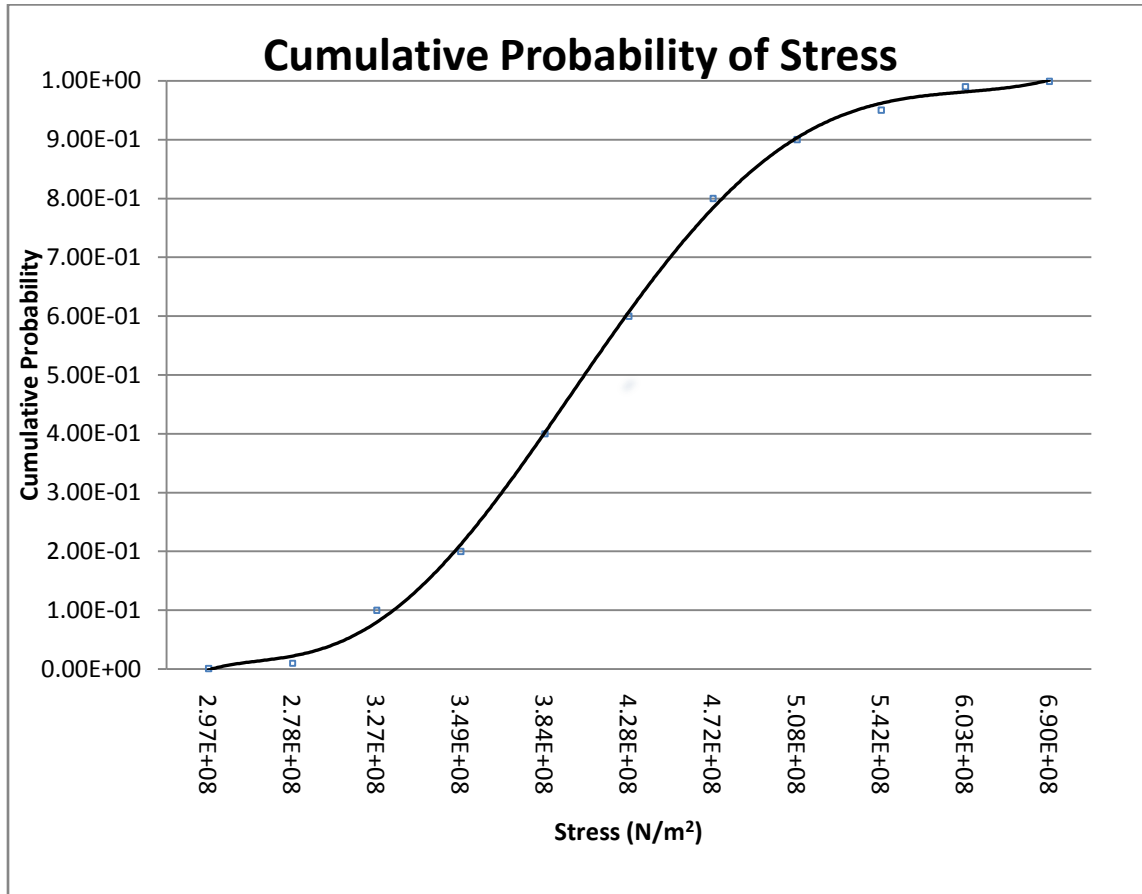Figure 16. Sensitivity factor versus random variables for probability = 0.999.

Figure 17. Cumulative probability of stress.

CHAPTER V

RESULTS FOR PROPOSED TANK SHAPES

The effect of noncylindrical walls on the maximum von Mises stress was examined for one radius of curvature of the tank walls. A tank with concave walls having a radius of 234.3m was studied in addition to the straight walled tank. Figure 18 and 19 shows the proposed view of the tank with concave walls.

In general, the stress of the concave-walled tank is lower than that of the straight-walled tank. This concave walled tank is a proposed design for LNG tank. The concave walled tank is similar to the shape of a hyperbolic cooling tower. The hyperbolic shape is selected to minimize the stresses. The stresses in the elongated shape concave tank has 30% lower maximum stress than the regular shape LNG tank.
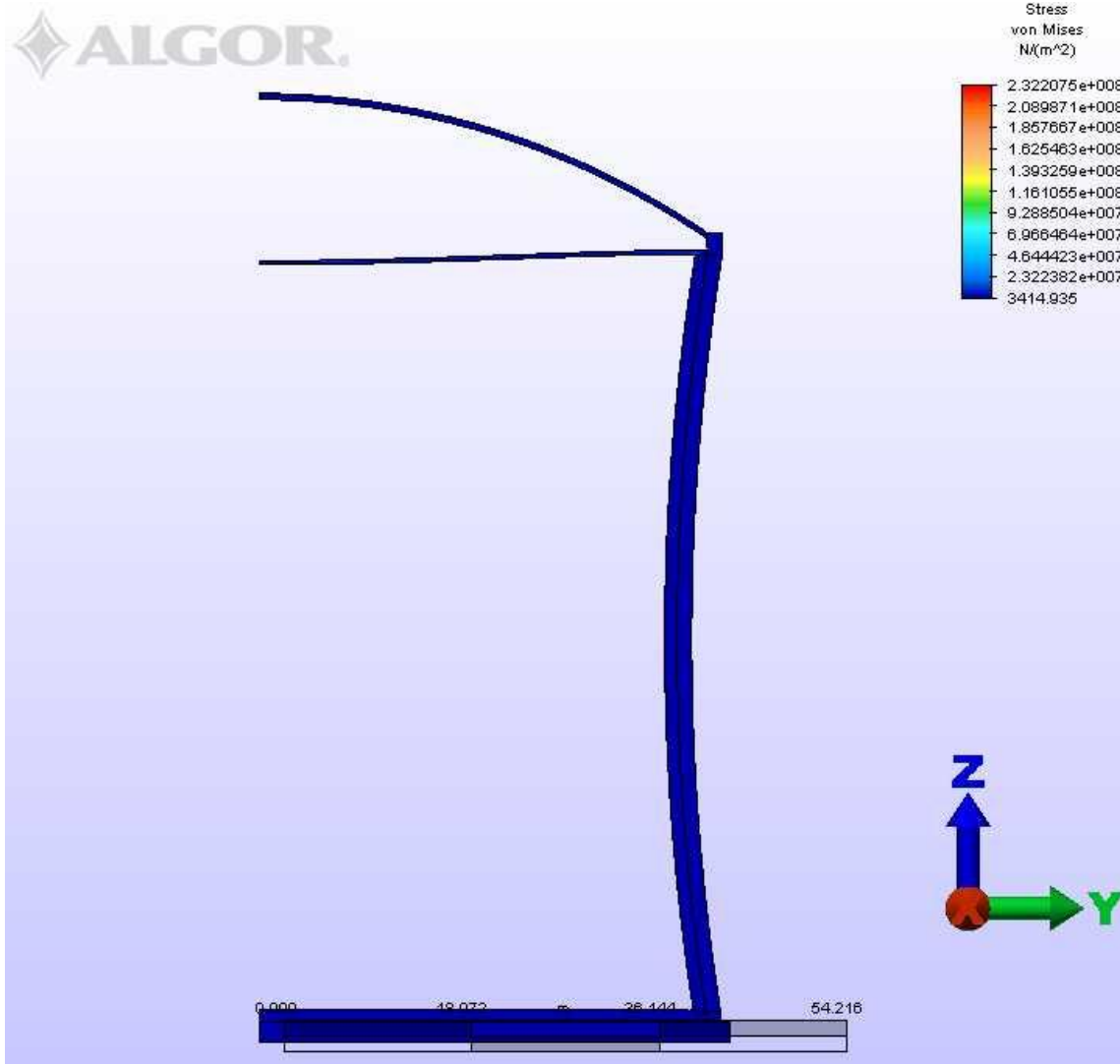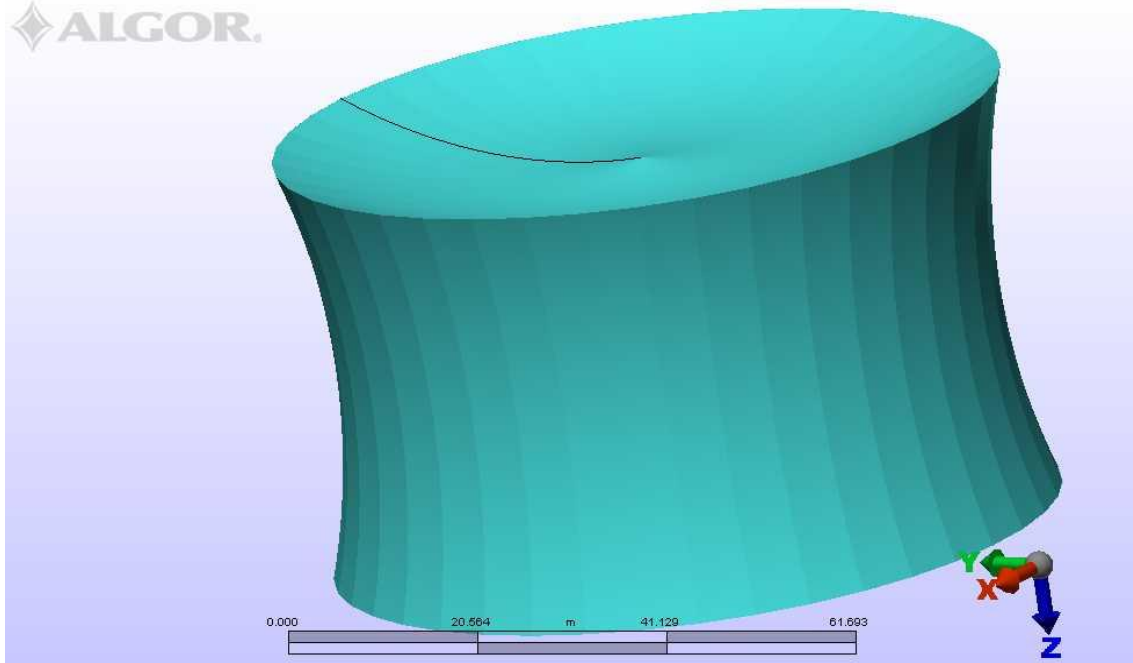
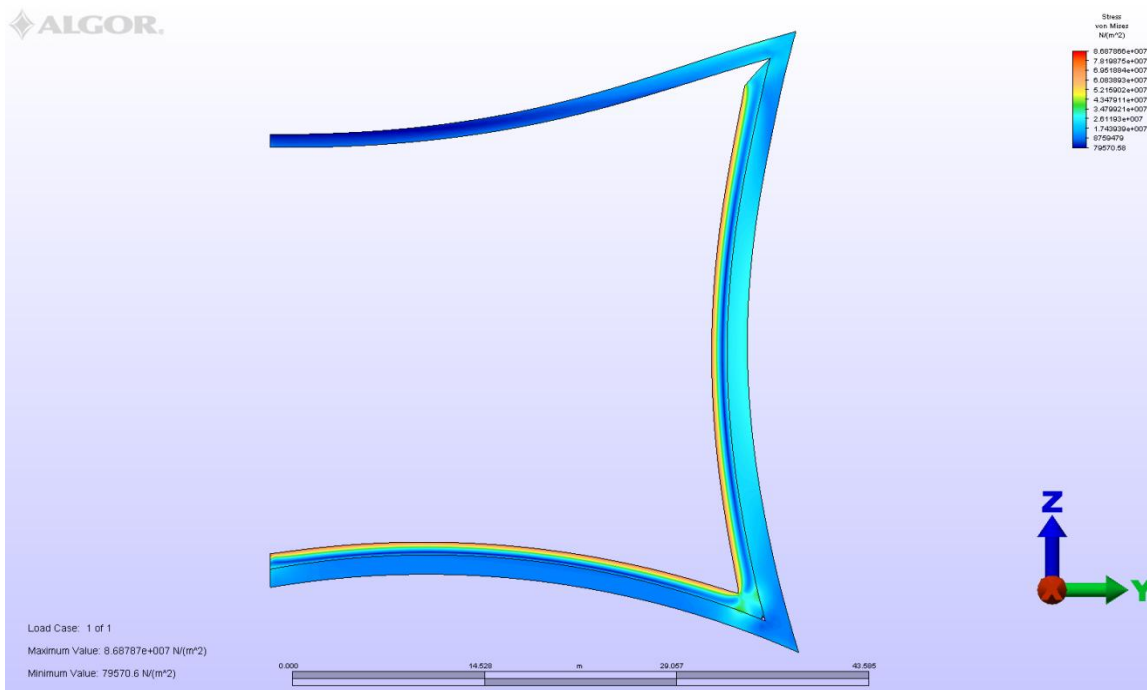Figure 18: Proposed shape for LNG tank

Figure 19: Concave wall

Figure 20: Stress results for concave wall

CHAPTER VI

CONCLUDING REMARKS

A full containment LNG storage tank—with typical dimension abstracted from several research papers---was modeled in ALGOR. The novelty of this thesis is the probabilistic evaluation of the finite element solution for a thermally and mechanically loaded cryogenic fluid containing enclosure. Cumulative distribution functions and sensitivity factors were computed for stresses generated due to 54 random variables in the areas of thermal, material, and structural variables that govern the LNG tank. Additionally, the boil off in weight percent of the tank per day was calculated at the mean of the random variables.

One aim of this thesis was to predict the uncertainty in the stresses of the LNG tank under non-ideal conditions due to variation in the random variables. The first step was to perform a finite element analysis using ALGOR to determine the maximum temperatures and von Mises stresses for each run. The NESTEM probabilistic engineering analysis software was then used to simulate uncertainties in the random variables. Probabilistic design is a way to formally quantify the effect of uncertainties. Probabilistic design is necessary because the effect of the variables on

maximum temperature and stress have to be described accurately. In sum, a design can be cost effectively accomplished if the effects of uncertainties are known.

The rate of boil-off per day is 0.051% by weight found by calculation in this analysis is within the range found in the literature for similar sized LNG tanks.

The sensitivity factors versus random variables for the probabilities from 0.001 to 0.999 were found and the longer bars in the plots indicated variables with a large impact on stress. All the variables have at least some effect on the von Mises stress whereas some variables have a high impact, which include the inner temperature, the coefficients of expansion of the base and side of the inner tank, inside convection coefficient, height of the tank, and the moduli of elasticity of the side and the base of the inner tanks. Most of the other variables have a much smaller contribution to the stress. Evaluating the sensitivity factors will enable the identification of the most critical design variables in order to optimize the design and make it more cost effective.

References

1. H. Lun, F. Fillippone, D. Cobos Roger, and M. Poser, "Design and construction aspects of post-tensioned LNG storage tank in Europe and Australasia", New Zealand Concrete Industry Conference, September, 2006.

2. Q-S. Chen, J. Wegrezyn, V. Prasad, 'Analysis of temperature and pressure changes in Liquefied natural gas (LNG) Cryogenic tanks", Cryogenics, vol. 44, 2004.

3. S.-J. Jeon , B.-M. Jin and Y.-J. Kim, "Consistent thermal analysis procedure of LNG storage Tank", Structural Engineering and Mechanics, Vol 25, No. 4. 2007

4. B. T. Oh, S. H. Hong, Y. M. Yang, I. S. Yoon, and Y. K. Kim, "The Development of KOGAS Membrane for LNG Storage Tank", Proceedings of the Thirteenth International Offshore and Polar Engineering Conference, Honolulu, Hawaii, May 25-30, 2003.

5. S. J. Jeon, C. H. Chung, B. M. Jin, and Y. J. Kim, "Liquid Tightness Design of LNG Storage Tank Incorporating Cryogenic Temperature-Induced Stresses"

6. M. Graczyk , T. Moan, and O. Rognebakke, "Probabilistic analysis of characteristic pressure for LNG tank", Journal of Offshore Mechanics and Arctic Engineering,Vol. 128,2005, pp. 128-133.

7. S.-J. Jeon and E.-s. Park, "Toward a Design of Larger Above-ground LNG Tank", LNG Journal, March/April.

8. Y. Yang, "Development of the world's largest above ground full containment LNG storage tank", 23rd World Gas Conference, Amsterdam 2006.

9. A. Bashiri, "Modeling and Simulation of Rollover in LNG Storage Tanks", International Gas Union 2006.

10. A. Salem, R.S.R. Gorla, "Probabilistic Finite Element Thermal Analysis Applied to a Water Tank Design", International Journal of Fluid Mechanics Research, Vol. 31, No. 2, 2004, pp. 131-142.

11. B. H. Thacker, D.S. Riha, S. H. K. Fitch, L. J. Huyse, and J. B. Pleming, "Probabilistic engineering analysis using the NESSUS software", Structural Safety, **28** (2006) 83-107.

12. R.S.R. Gorla, S.S. Pai, and J.J. Rusick, "Probabilistic study of fluid structure interaction", International Journal of Engineering Science, **41**, (2003), 271-282.

13. R. S. R. Gorla, N. R. Gorla, "Probabilistic finite element analysis in fluid mechanics", International Journal of Numerical Methods for Heat & Fluid Flow, **13**, No. 7, (2003) 849-861.

14. R.S.R. Gorla, and O.Haddad, "Finite Element Heat Transfer and Structural Analysis of a Cone-Cylinder Pressure Vessel", International Journal of Applied Mechanics and Engineering, Vol. 12, 2007, 951-963.

15. J. P. Holman, Heat Transfer, McGraw-Hill, Tenth Edition, 2010, 332-350.

16. T. Kanazawa, K. Kudo, A. Kuroda, and N. Tsui, "Experimental study on heat and fluid flow in LNG tank heated from the bottom and the sidewalls", Heat Transfer—Asian Research, **33**, 2004, 417 – 430.

17. Southwest Research Institute, "Probabilistic structural analysis methods (PSAM) for select space propulsion system components", Final Report NASA Contract NAS3-24389, NASA Lewis Research Center, Cleveland, OH; 1995.